Machine Learning for Mobile Applications:

Leveraging A DNN For AoA Estimation And User Localisation In mmWave Netwroks

---

Department: School of Engineering and Informatics

Candidate Number: 230890

Supervisor: Dr Falah Ali

Degree Course: Electrical and Electronics Engineering with Robotics

(B.Eng.)

Word Count: 7,400

SUMMARY

With the advent of the 5th Generation (5G) of telecommunication technology and the annually increasing growth of mobile/wireless devices/traffic, intensive research is being conducted to build wireless technology that may be able to effectively cope with the higher data rates and traffic of the future. mmWave networks are a forerunner technology for this. mmWaves grant access to unprecedented spectrum. However, mmWave networks will require effective beamforming techniques in order to deliver efficiently, the demands of future mobile traffic. Traditional beamforming is costly and consumes large overhead. In this report, based on recent research, I design and test a basic feed forward Deep Neural Network (DNN) for Angel of Arrival (AoA) estimation and user localisation, that a may be leveraged by a beamformer to produce the optimal beam vectors for users. The data for the DNN is generated using the DeepMIMO dataset generator. The results show that the DNN performs well for AoA but due to lack of optimisation the DNN does not perform as well for user localisation.

STATEMENT OF ORGINALITY

DECLARATION:
In making this submission I declare that my work contains no examples of misconduct, such as plagiarism, collusion, or fabrication of results.

I confirm that I have talked with my project supervisor about whether ethical review will be required, and that the outcome of the discussion is included in my interim report.

Should ethical review be required, I confirm that I will submit an application before the end of the autumn term. Furthermore, if the ethical implications of my project change, I confirm that I will alert my supervisor immediately.

SIGNATURE:

TABEL OF CONTENTS

ACKNOWLDGEMENT

My path towards the completion of this dissertation was not straightforward. I owe Dr Falah a debt of gratitude because Dr Falah, with his grand experience and exhaustive knowledge of the field of study-this dissertation is concerned with-guided me and helped me.

I wish to thank my parents and my grandfather, who all, after enduring one of greatest losses of their lives, continued their steady and unconditional support for me during my time spent at Sussex.

To all,

I am grateful.

1. INTRODUCTION

1.1. Background:

ML has become a primary tool that serves humanity in nearly all fields. ML systems employ algorithms that utilise the available data and measurements in order to optimise the performance of systems. This motivates their applications in the mobile/wireless communications field. The number of mobile devices ergo the data transferred every day is increasing [1]: the telecommunications company Ericsson stated in its 2021 report, whilst reflecting on the past decade, that there were, by the end of 2021, nearly 4.7 billion 4G subscriptions, 5.5 billion new smartphone subscription and that mobile networks carry nearly 300 times more data traffic than they did in 2011. The report also forecasts that by the end of 2022 there will be 660 million 5th Generation (5G) subscriptions and that the growth of 5G devices will be faster than that of any other mobile technology in the past. Also, that massive Internet of Things (IoT) will make up 51% percent of the IoT connections in the world by 2027.

This significant growth increase in the wireless and mobile devices reflect very well upon how such technology have been integrated into human life considering their application. Such applications have high data rates and need real time and swift responses in order to work efficiently and effectively. Most systems employed, in order to either, solve network issues or enhance network performance, make many assumptions about the system. Such assumptions ignore the dynamic behaviour of the mobile networks especially in this age when they are constantly evolving and their complexity increasing. Existing networks lack the intelligence required in order to serve future next generation networks effectively [2].

The burst of growth in the mobile data sector and the intensive use of smart devices along with the introduction of wireless IoT (Internet of Things) connections have also caused a global bandwidth shortage [3]. The global cellular providers are limited to the bandwidth of 700 MHz – 2.6 GHz, this is a hindrance in their goal to provide high quality, minimal latency, audio, video and multimedia applications. The high-density networks also cause high path loss, diffraction losses and signal distortions at high frequencies, the use of multi antenna systems has become a necessity [4].

This has motived the development of telecommunication systems that may be able to, efficiently and effectively, serve such a dense network; mmWave systems are a forerunner technology in developing such systems. They occupy a large bandwidth range, 30-300 GHz, which makes them a reliable solution to tackle such high data rates. Their short wavelength

also allows the deployment of large antenna arrays and provide narrower than sub-6 GHz frequencies. This has made mmWave communication systems a key technology in the fifth generation (5G) and beyond of wireless communication [5].

mmWaves have attracted the attention of researchers recently, due to their large Bandwidth. For mmWave systems the rates are far better than that of lower frequency devices [5]. The hardware of the mmWave systems provides certain advantages over conventional microwave systems, also, the shorter wavelength makes it possible to deploy antennas at, both, the transmitter and receiver. The large antenna arrays motivate the use of Multiple Input Multiple Output (MIMO) techniques which increase spectral efficiency along with being able to employ direct beamforming which increases signal power and decreased interference [6]. However, most research till now has been focused on low mobility systems. High mobility mmWave systems enable many applications e.g., vehicular communication, mobile virtual and augmented reality systems. These applications are especially data hungry and require high data rates for optimal connectivity and Quality of Service (QoS). The mmWave band characteristics give rise to certain challenges when dealing with such applications scenarios also has an adverse impact on signal reliability: mmWave systems require frequent handover from Base Station (BS) to BS: the narrow beams are sensitive to blockage which impacts their coverage, reliability and causes latency issues during highly mobile communication [7].

Due to these constraints the use of multiple antennas-MIMO-at the transmitter and receiver location has been the key implementation technology in mmWave systems . Their small wavelength has enabled the packing of many antennas into small spaces which further enables, having many of them in small handheld devices or in small cells at the BSs which enables the use of massive-MIMO, a key architecture in 5G and beyond communication. In such architectures beamforming, beam tracking and beam alignment are key parameters that need to be perfected in order to make a robust and reliable system, as they provide effective solutions to the mentioned constraints by establishing and maintaining the communication link [4].

Effective beamforming is dependent on acquiring accurate information of channel parameters such as, the Angle of Arrival (AoA), Angle of Departure (AoD) and other channel information. These variables are constantly changing in high mobility systems. In order to maintain an effective link with the user, the system must be able to track the location, learn the correlation between its mobility and the channel parameters and then be able to

predict the trajectory of the users. Traditional algorithms have some constraints which are bound to become more problematic with the increasingly complex systems that also are dynamic in character; such algorithms have a set of pre-programmed instructions that they use to process data, manage and operate the systems [4].

These may be replaced by ML algorithms which are formed based upon real life data acquired in real time. ML is a subset of AI that may be integrated into such systems. ML develops algorithms that mimic the learning and problem-solving capabilities of the human brain. ML algorithms are dynamic; they are able to process data and learn from it as it changes.

ML learns through the training data that is input to the algorithm. This data is utilised by the algorithm in order to produce a set of rules, based on inferences from the data which results in a new algorithm. Thus is MLs' ability to process dynamic data accurately. ML application consist of two phases: training and decision making. During the training phase ML techniques use the training set to learn the model. For the decision-making phase, the algorithm outputs, for each input, an estimate based upon the training data [8].

1.2. Objectives:

The objectives of this report are:

1. To acquire a dataset that provides accurate/realistic data about mmWave networks.
2. Use the dataset to generate channel between User Equipment (UE) and BS in a high mobility scenario
3. Design/Build an basic ML model that is able to utilise parameters from the generated channel in order to make estimates about user AoA and location; information that can be fed to a beamforming system.

2. LITERATURE REVIEW AND THEORY

2.1. mmWaves and Beamforming:

The 5G of cellular communication networks is shifting towards technologies that aim to employ mmWave frequencies [7]. This shift will provide multi-Giga-bits-per-second (Gbps) data rates to the UE and access to spectrum that has not been utilised till now. Channel Bandwidth for 5G mmWave communications will be tenfold of the current 4G Long Term Evolution (LTE) channel today, at 20 MHz [9]. [10] carried out an analysis that shows that a channel with a width of 1 GHz may offer several Gbps of data rates to UE with phased array antennas, at 28 and 73 GHz. While [11] and [12] show in their results that, for UE employing 4x4 phased array antennas, it is possible to reach 15 Gbps data rates at a distance of 200m from the BS.

However, providing such rates with effective communication links in real scenarios with mobile users becomes a challenge. To cope with this issue, effective beam forming is required. [13] and [14] explore different technologies that are able to read the channel parameters such as AoA and power, then, use them to form a channel vector. The traditional techniques, employed in these papers, such as Kalman Filter (KF) and training RF beamforming to through a comprehensive search to find the best vector, do provide satisfactory results, they require huge training overhead and would be unable to fully and properly capture the channel dynamics of the high mobility mmWave systems.

2.2. Machine Learning:

ML is chiefly divided into three subdivisions: supervised learning, unsupervised learning and reinforcement learning (RL). RL employs techniques from both supervised and unsupervised learning. Another type of learning, Deep Learning (DL) is commonly encountered when going through ML literature. DL is not classified as a separate subdivision of ML as it may be applied to any of the subdivisions stated above by simply adding a Deep Neural Network (DNN) to their structure. A common way of describing an ML framework is one that consists of a model, optimisation algorithm, loss function and dataset [5].

[5] states that a program is said to learn when its performance at some task T improves, as measured by a performance criteria P, for each experience E. Tasks, performance criteria and experiences vary in accordance with the ML algorithm type and its application. E.g., a classification task would assign a class label to an input or data structure, different objects within the data might give rise to different labels but the process for assigning them is the same. A regression task, however, would assign a real value to an object within a dataset.

The performance criterion is used to evaluate the learning algorithm. It may be a calculation of the accuracy of the algorithm e.g., in the case of classification it may the measurement of how many objects in the data the correct labels are assigned to divided by the total number of inputs. The experience of the learning algorithm classifies it into one of the ML subdivisions.

2.2.1. Supervised Learning:

In the supervised learning framework, the algorithm is provided a dataset that contains objects and their respective labels or targets. Supervised learning attempts to predict the target for the object after learning. E.g., if an object in the dataset is denoted by *a* and has a target or label *b,* this will form a training example (*a,b*) within the dataset. The algorithm will then estimate the probability $p(a|b)$, from which it may be able to make an accurate prediction of a label *b* for an object *a.* Some of the most common used supervised learning algorithms for classification and modelling existing datasets are Support Vector Machines (SVM), Naïve Bayes Classifier and Decisions Trees (DT). DTs may also be used for regression. In mobile/wireless communications these algorithms are most commonly used for localisation, channel estimation and spectrum sensing [5],[15].

2.2.2. Unsupervised Learning:

This sort of learning algorithm is provided with an unlabelled dataset without the target outputs. Hence, it learns the regularities within the dataset that may seem useful instead of simply mapping inputs to specific outputs. This may be done by looking patterns within the dataset that occur more and understand what does and does not happen. This is known as density estimation in statistical terms. This sort of learning is especially useful when working with a system that produces datasets without targets, as it would be impractical for a human to through and label the whole dataset. This also motivates the algorithm to present the data in a simpler manner [5],[15].

The loss functions used for unsupervised learning are different from those in supervised learning algorithms. The best type of loss function is one that makes the algorithm preserve the information about the input and present the data in a simple manner. The Principal Component Analysis (PCA) and K-mean clustering are the commonly used unsupervised learning algorithms. In mobile/cellular networks unsupervised learning is used mostly for clustering, probability density estimation and denoising problems [5].

2.2.3. Reinforcement Learning:

RL combines techniques from both supervised and unsupervised learning. The framework of an RL program can be described by an agent, a policy and the environment. The output for such a framework is not a single action but a series of actions that reach the desired output. In this the policy determines the course of actions that the agent must take in order to the goal. During the process the agent receives reward signals from the environment which determine how well the agent is doing at that given time step, the reward signal itself define the ultimate goal of the algorithm. The agent then, takes into consideration its observation of the environment and the reward signal, in order to decide the actions, it must perform on the input and maximise its long-term reward. Q-learning is a common RL algorithm. This sort of behaviour makes RL suitable for application with networks that are dynamically changing; it may be used for IoT devices or for spectrum sharing and BS association in cognitive radio networks and small cell area networks [2],[5].

2.2.4. Deep Learning:

Deep learning is based on Artificial Neural Networks (ANN). DNNs consist of several layers which are, the input layer, the output layer and hidden layers between them. When training on a dataset, DNNs are able to approximate a functional relationship that exists between the data in the dataset. The functional relation is general and may be applicable on data points not in the dataset. Each layer consists of a specified number of neurons which activated due to excitation. This process is meant to imitate the perception processes of a human brain. Fig.1 shows an example of a common multilayer neural network. The input layer has three nodes (neurons), representing three inputs, the inputs are fed into each of the nodes on the first hidden layer and then the output of their nodes into each of the following, until the output from the last hidden is fed into the nodes of the output layer to provide two outputs [16], [5].

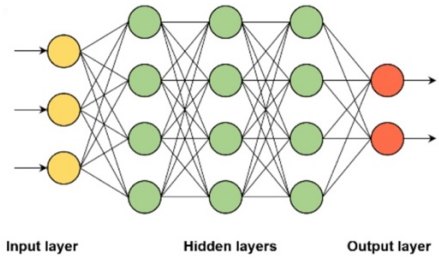

(Fig.1)

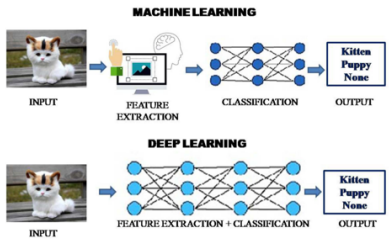

(Fig.2)

DL has several advantages over ML. DL is able to, automatically, extract high level features from the input data. Therefore, there is no need for humans to build multiple non-linear

layers for the learning model. Fig.2 shows an example of how a DL model would perform the same image processing task in comparison to an ML solution. In this example the DL algorithm will extract features in layers, i.e., the first layers would extract complex base level features like processing the digitised pixels to extract the colour. The outputs from this layer will be input to the next, which will make use of them to extract more complex features. The output of each layer will be input to the next until the final layers which will process the image based on all the different features extracted and input to it and classify the image to be a certain category [5]. This simplification and automation reduce the computational complexity and also saves time as the same trained model may be used for several tasks without any changes being made. Also, DL is able to process large amounts of data and is scalable with increasing data.

Multilayer Perceptrons (MLPs) also known as feedforward neural networks are one of the most common and useful architectures that implement deep learning. In fact, the architecture and data processing procedures of feed forward neural networks give rise to the term deep learning. The main objective of a feed forward neural is to build function *f* that maps an input *x* to an output *y*. During the mapping the NN also learns parameters θ that result in the best function *f*. The mapping may be summarised using (1) [16]. Every neural network has parameters and hyperparameters. Parameters of a NN are coefficients that need to be only initialised by the user, they are updated/optimised by the model itself in order to reach the optimal output. The hyperparameters, on the other hand, must be optimised by the user themselves. Examples of hyperparameters are activation functions, optimisers, number of hidden layers and learning rate. These may optimised through extensive trial and error or by using automatic optimiser that employ several combinations of hyperparameters, then, based on performance output the most optimal combination.

$$\boldsymbol{y} = f(\mathrm{x}; \theta) \quad (1)$$

This is especially useful in mobile/cellular networks as it may be able to serve in building an appropriate function approximation between the channel parameters (such as the path power, path loss, ToA) and the AoA and locations of users (16).

2.3. Challenges faced by ML application in mmWave:

One major challenge that the application of ML faces in mmWave systems is the availability of data sets. ML requires large datasets that the algorithms require for training and learning purposes. The data must also be labelled in order for supervised learning algorithms to make good use of it [17].

Acquiring real, labelled data can be a costly and time-consuming process and at all not feasible for small scale research. For this reason, a few datasets have been published that generate synthetic data based on real scenarios [18]

2.4. Review of Related Literature:

In [19] the authors use both a ML and DL technique in order to estimate the AoA of UE. The ML approaches used are the Support Vector Classifier (SVC) and the *k*-Nearest Neighbour (kNN); for the DL approach a Multi-Layer Perceptron (MLP) type, feed forward NN, is used. The ML and DL models are integrated within an Analogue Beam Former (ABF). The goal is for the ML and DL model to utilise an estimate of the AoA and received signal power of the UE; the output is the optimal formation for the ABF. The benefit of this is that it avoids the costly exhaustive search routine for every ABF in the codebook. In their results they show that the DL solution, the MLP, outperforms the ML solution by estimating the AoA and received power by an accuracy of 80%.

The authors of [20] aim to propose a system that may be able to improve user localisation in order to implement faster beamforming to cope with greater data rate and coverage in 5G networks. For this system a DNN is used to localise User Equipment (UE) in two static scenarios at mmWave and sub-6 GHz frequencies and explains the effects of using different channel parameters to train the network. They take two different approaches to train the DNN, the first approach uses raw channel parameters such as the AoA, Time of Arrival (ToA) and Received Signal Strength (RSS) as learning features; the second approach uses the channel response vector. The output labels for both approaches are the x and y location of the user. The data is generated using a ray tracing simulator, REMCOM wireless Insite []. For the first approach a scenario is considered in which multiple BS nodes and UE grids are setup in an urban environment. The BS nodes employ half-wave dipole antennas and are located at a height of 10m from the ground with a transmission power level of 0dBm. A total of 1530 UE receiver points are simulated, the location of the UE in their respective grids are the output labels of the DNN. For the second approach a scenario is considered where UEs are made to communicate with different BSs. The channel vectors are built for 185 simulated

users. The DNN design has two hidden layers for both approaches. The hyperparameters are optimised using Bayesian optimisation by calculating the Mean Squared Error (MSE). For the first approach 3 sets of inputs are used each with more input learning features. The results for both, the mmWave and sub-6 GHz frequencies, show that by inputting more training features, the accuracy of the DNN increases. For the second approach the DNN is trained with the channel response vectors of the simulated users, the results show that the DNN does not train properly as the spacing between the users is 1 meter hence, the vectors are very similar.

The work in [3] aims to address the issue of the need of beam tracking in multi antenna mmWave networks due to channel impairments such as diffraction and high path loss because of high frequencies. The authors aim to explore a ML solution for tracking the AoA at the UE in order to maintain a communication link between BS and UE. The main motivation to use a ML approach is due to its Universal Approximation property that enables it to accurately capture the channel and environment of dynamic networks. Also, a trained ML solution only requires base level mathematical operations that can be performed in real time. Both such qualities serve as a major advantage over traditional algorithms that require intensive calculations and make assumptions about the network that do not fully capture the dynamic behaviour of the network.

The scenario considered is one where an omni-directional BS is communicating with a UE equipped with a Uniform Linear Array (ULA). The assumptions made are that an initial connection has been established between the UE and the only problem to be tackled is to maintain that link. The data for this study is generated using the QuaDRiGa framework [21]. A Non-Line of Sight (NLOS) urban micro-cell environment within the framework is considered. A cell has a BS equipped with one omni-directional antenna with a carrier frequency of 28 GHz. 2500 realisations of UE mobility are generated with each being 20 m long. The AoA and channel coefficients are recorded every 0.1 m of every path realisation. The authors propose a model that uses a Neural Network (NN) to track the AoA at the UE side. The RNN has a fully connected layer with 20 neurons, followed by an LSTM layer with 40 neurons and another fully connected layer with 20 neurons at the end. The inputs to the NN are the observed noisy signal (SNR) and an estimate of previous AoA. The output is an estimate of the AoA at the current time. During testing a certain threshold for AoA is set, compared to which if the difference between observed and the predicted AoA is greater, the user announces outage, i.e., the AoA is too large for the user to maintain the connection. This assumption is important, as a metric called the outage probability is used to analyse and

evaluate the results of the ML model: outage probability in mobile/cellular communication may be defined as a point after which the receiver is not on range of the BS or in technical terms the receiver signal power has fallen below a set threshold and the connection is broken [22]. A comparison is made between the ML and a traditional Kalman Filter (KF) based approach; the outage probability is plotted against the SNR. The ML solution shows lower outage probability for lower an SNR but converges with the KF based approach when SNR is high. This clearly shows the advantage of using ML to make a prediction of AoA. The results also represent that the ability to track the user AoA of the UE is imperative to maintaining a robust connection with the UE in order to provide it a good QoS.

The authors of [6] integrate a ML model within a beamforming system which helps maintain the connection between the BS and UE also, this maintains an optimal data rate. They propose a DL coordinated Beamforming solution in order to enable efficient communication for highly mobile mmWave systems. The proposed solution considers a scenario where multiple BSs are serving the same mobile user. The user is required to transmit one uplink pilot sequence from which the BSs simultaneously draw a signature for the users' location and its interactions with the surrounding environment. This signature is utilised by the DL model in order to predict the optimal beamforming vectors for the user. The DL coordinated beamforming solution is compared against a base-line coordinated beamforming solution, that does not use ML and a Genie-Aided beamforming solution that already known the optimal beamforming vectors. The metric used for comparison is the effective achievable rate; this metric takes into account the computation time taken in designing the optimal beamforming vector and the data rate that it achieves. Even with increasing dataset size the DL coordinated solution outperforms the baseline coordinated beamforming solution by reaching almost optimal data rates. A similar experiment is conducted by [] where a NN is used to predict the channel information of a user based upon the past Channel State Information (CSI). The purpose of this experiment is to propose a design that may be able to provide a stable link between BS and mobile UE. Their system considers that all BSs are connected to central cloud. When the pilot is received from the UE at all BSs simultaneously, the channel vector is sent to the cloud process which integrates all the channel vectors into one. Using the integrated channel vector, the ML model makes a prediction of the CSI which is sent back to the BSs which use this information to form the next channel vector. This removes the need of the BS to perform channel estimation. The results of the ML model are analysed using the normal mean squared error between the estimated and predicted channel; the error between the estimated and predicted channel is almost negligible after the NN is

properly trained. The successful results of both ML models may be attributed to the similar structure and hyper parameters that they have. Both structures employ online learning in order to train the NN and use a multi-layer structure.

The simulation carried out by [23] provide further results that may be used to enhance the performance of ML models in mmWave systems. The authors carry on work on the system mentioned previously in the work of [6]. Instead of building on it, they try to optimise the performance of the system by employing different optimisers in the NN. Their results found that using both, the adam optimiser, as was used by [6] and a variant of it, Nadam, provide optimal results in NN performance in predicting the channel parameters used in building the channel vector.

The overview of the literature provides a comprehensive analysis of the constraints that traditional beamforming techniques may encounter in high mobility mmWave systems. To tackle these constraints this report aims to produce a low-complexity DNN at the BS end that is able to utilise channel parameters from the incoming path of the UE in order to perform user localisation and AoA estimation. This information can be leveraged by a beamformer in order to build a channel vector going out to the UE. This can avoid the exhaustive and intensive search procedure that traditional beamformers go through in order to build the optimal channel vector. Thus building a more reliable system.

3. METHODOLOGY AND PROJECT DESIGN

This section gives an overview of the methodology employed in the research, design and simulation process of the project.

3.1. Methodology Employed to Achieve Project Objectives:

The very first task undertaken was to gain a basic understanding of ML techniques and their application in the mobile communication sector in general. This was done by reading significant theoretical literature available on the internet. The focus was then turned to a specific part of mobile communication, as is apparent by now, mmWave networks have been the point of focus due to their expected application and usefulness in progressing the evolution of mobile communication. Whilst going through previously conducted experiments to choose an appropriate application for ML in mmWaves, the following criteria was followed:

1. Is the difficulty of the application suitable for my level of study and knowledge?
2. Does it have wide scope in the future?
3. Is it a field I would want to pursue in the future?
4. Are there enough resources, at my disposal or on the internet, to conduct this study?

Leveraging a DNN to predict the AoA and location of UE filled all the criteria very well. After the finalisation of my topic the first- and most-time consuming task was to acquire a dataset that would simulate accurate UE realisations. After finding an appropriate dataset, a simple NN structure was built, an MLP. Details about both, the dataset and the NN structure, are provided in the following subsections. A thorough logbook for this project was not possible as it is dominantly software based.

3.2. Project Design:

Utilising real world data is they most accurate method for the design and testing of a system. This, however, was not a feasible approach for my level of study. My second-best option was to look for a dataset in which the generated data captures the effect of the environmental setup on the generated channels. For this reason, the DeepMIMO dataset is chosen [18]. The DeepMIMO dataset generates channels based upon accurate ray-tracing data from Remcom Wireless InSite [24]. Another advantage of this dataset is that it is flexible. Meaning that it allows the user to manipulate the main system and channel features/parameters to generate data bespoke to their application. The generated dataset consists of the raw channel parameters and the location of users which form the inputs for the DNN. The inputs are

utilised in two different approaches, the first is meant to estimate the AoA based of user location and channel parameters. For the second approach the raw channel parameters are used to carry out user localisation (finding the location of the user).

3.2.1. Dataset Description:

The DeepMIMO dataset is also used by [6] and [20]. A visual representation is provided in Fig. The dataset generation code takes in two inputs, the scenario and parameters. The ray-tracing scenario may be outdoor or indoor, it has a certain number of BSs and users that are geographically distributed. The outputs include the channel parameters for the channel that exists between each user and BS (transmitter and receiver). The parameters are set by the user.

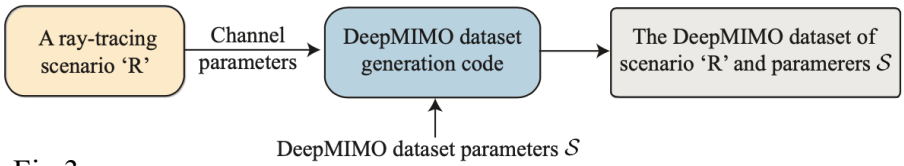

Fig.3

Scenario: From [18] the 'O1' ray tracing scenario is chosen. The scenario is provided by Wireless Insite, a ray-tracing software by Remcom [24]. This is an outdoor scenario as shown in Fig. It consists of two streets, the vertical street is 440m in length and 40m in width, while the long/main street is 600m in length and also 40m in width. The total number of BS available are 18, with a distance of 100m between each in the main street and 150m in the vertical street. The BSs, each, have a single antenna in the z direction with a half wave dipole. However, the code for the generating the dataset has mathematical functions that enable the users to generate channels for larger antenna array at the BSs.

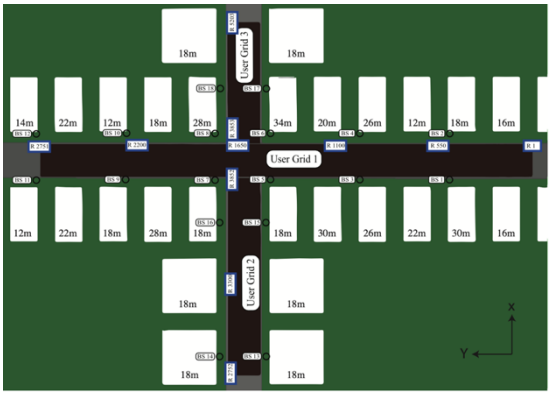

Fig.4

Each building in the main street has a base of 30x60m wile each building in the vertical street ism has a base of 60x60m. The heights of the buildings are in Fig. The materials used are ITU 60 GHz glass, ITU 60GHz single-layer dielectric for the ground and 3-layer di-

electric ITU 60 GHz for the buildings. The dataset generates users in rows, each row has 181 users. The main street has 2751rows, meaning it can simulate a total of 497,931 users there. The rows are set in the x direction, i.e., the distance between each user within a row differs by 0.2m in the x direction whilst remaining on the same y coordinate. Each user has a single dipole antenna, which is assumed to be at a height of 2m, whilst the BS are assumed to be at a height of 6m from the ground (in the z direction).

The ray tracing simulator shoots many rays in all direction for every transmitter and receiver pair, it then records the 25 strongest paths based on their receive power strength. For every transmitter (BS) and Receiver (user), the simulator generates the raw channel parameters for every existing channel. The raw channel parameters are the path phase, the path power, the propagation delay of the path/Time of Arrival (ToA), the azimuth and elevation angles of arrival and departure.

The dataset generation code then uses the ray tracing simulator outputs to generate the channel vector for every BS and user channel according to equations mentioned in [25]. Along with this the dataset also outputs the x,y,z location coordinates of a user on the grid.

The parameters used to generate the dataset for my application are summarised in table 1 and figure 5 shows the part of the scenario considered for the formation of the data set. All channels are produced at a 60 GHz frequency.

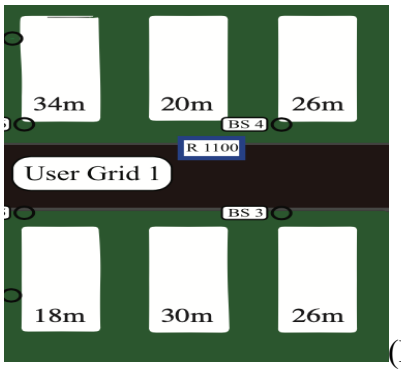

(Fig.5)

Active BSs	3,4,5,6
Users	Row 1000 to 1300
Number of BS antennas	Mx = 1, My = 32, Mz = 8
System Bandwidth	0.5GHz
Number of paths	1

The parameters used are the same as the ones used by [6] and [20]. For the sake of simplicity only the strongest path is considered. Furthermore, the channel parameter values and locations are recorded for channels between BS3 only and the 180 users with varying x-direction and y-direction. The distance between each user is 0.5 meter

3.2.2. The NN Architecture:

The DNN architecture is an MLP or a feed forward neural network. The architecture consists of an input layer an output layer and two hidden layers between them. The AoA estimation and user localisation problems are tackled as regression problems. The architecture of the NN is inspired by those used in [20] . Two approaches are taken to carry out the simulations. Both approaches generate results for three different sets of inputs.

For the first approach the inputs are the users x,y location and channel parameters, which are, the user path power, phase, loss and ToA. They are used in three sets:

1. x,y location (2 inputs)
2. x,y location, path power and ToA (4 inputs)
3. x,y location, path power, ToA, path loss and phase (6 inputs)

The output labels are an estimate of the azimuth and elevation AoAs.

For the second approach the inputs are the azimuth and elevation AoAs, path power, phase, loss and ToA. They are also used in three different sets:

1. Azimuth and elevation AoAs (2 inputs)
2. Both AoAs, path power and ToA (4 inputs)
3. Both AoA, path power, loss, phase and ToA (6 inputs)

The output labels for this approach is the users x,y location.

The data for both applications totals a number of 366 users. 181 with varying direction in terms of the x axis and 185 with varying direction terms of the y axis. The data was collected in this way so that the NN could map the effects of mobility in any direction and return accurate values in dynamic scenarios. The NN is trained on 85% of the data and tested on 15%.

The hyperparameters of the neural network were decided after testing several combinations that have already been used in the reviewed literature. The two-layer architecture is adopted from [20]. A mean squared error (mse) loss function is applied, as this is a common choice in regression problems. Afterwards a few optimisers are tried in order to see which one delivered the lowest mse. The adam optimiser is chosen.

The mse is a function that takes the difference between a target and a label (input and target output), squares the difference, does this for every target and label in a dataset, divides it by the number of observations in a dataset [26].

The DNN is constructed in a Python environment using a tensorflow and keras libraries [27]. To follow the progress of the NN, the mean absolute error (mae) and the root mean

squared error (rmse) calculated and displayed. Both these values are negative oriented, i.e., the lower they are the better. However, mae is measurement of the magnitude of the errors in prediction set; it takes the sum of the absolute value of the difference between each prediction and actual value, it is averaged out over the whole dataset and calculated according to (2). Rmse, on the other hand, takes the square root of the sum of the squared differences between the actual and the predicted values divided by the observations in the whole dataset and is calculated by (3).

$$MAE = \frac{1}{n}\sum_{i=1}^{n} |y_j - \hat{y_j}| \quad (2)$$

$$RMSE = \sqrt{\frac{1}{n}\sum_{j=1}^{n}\left(y_j - \hat{y_j}\right)^2} \quad (3)$$

RMSE, due its mathematical model, gives significantly more weight to greater errors. Hence, for this application the RMSE value is a more desirable for the evaluation of the NN, as in this case any large error value is undesirable. The MAE value is still utilised as it provides an important comparison. As the difference between RMSE and MAE reduces, it indicates that the error magnitude is more or less equal throughout the dataset. If RMSE and MAE are both large values it means that the error are all equally great. If RMSE and MAE approach zero, this means that all the errors are of similar minute magnitude. This metric may even be provide aid in tuning hyperparameters for small scale ml applications. The DNN code and datasets are in available in the appendices.

4. RESULTS

This section presents the results from the simulations. In this section the word AoA is meant to represent both the azimuth and the elevation AoA. For the first approach the DNN is meant to predict the AoA based on three sets of inputs. The results are shown in graph 6, 7 and 8.

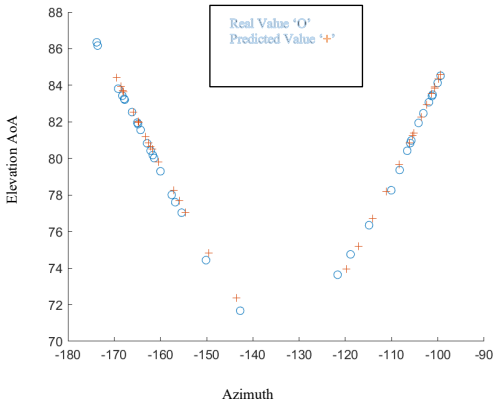


```
MAE: 1.867
MSE: 48.638, RMSE: 6.974
Model: "sequential"
_________________________________________________________________
Layer (type)                 Output Shape              Param #
=================================================================
dense (Dense)                (None, 8)                 24
_________________________________________________________________
dense_1 (Dense)              (None, 50)                450
_________________________________________________________________
dense_2 (Dense)              (None, 2)                 102
=================================================================
Total params: 576
Trainable params: 576
Non-trainable params: 0
_________________________________________________________________
```

(Fig.6, AoA predicted using only x,y location of user)

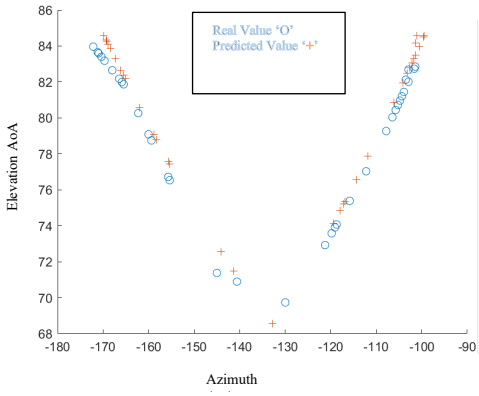


```
MAE: 1.328
MSE: 2.341, RMSE: 1.530
Model: "sequential"
_________________________________________________________________
Layer (type)                 Output Shape              Param #
=================================================================
dense (Dense)                (None, 8)                 40
_________________________________________________________________
dense_1 (Dense)              (None, 50)                450
_________________________________________________________________
dense_2 (Dense)              (None, 2)                 102
=================================================================
Total params: 592
Trainable params: 592
Non-trainable params: 0
_________________________________________________________________
```

(Fig.7, AoA predicted using x,y location, path power and ToA)

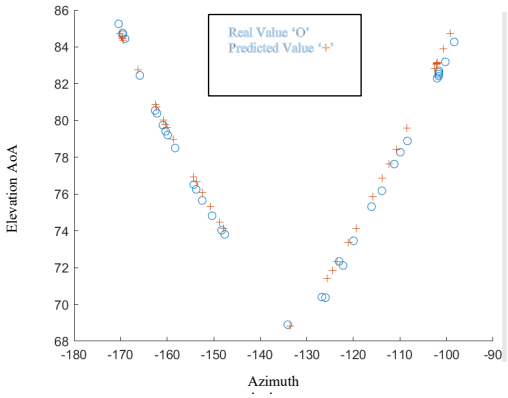


```
MAE: 0.461
MSE: 0.384, RMSE: 0.619
Model: "sequential"
_________________________________________________________________
Layer (type)                 Output Shape              Param #
=================================================================
dense (Dense)                (None, 8)                 56
_________________________________________________________________
dense_1 (Dense)              (None, 50)                450
_________________________________________________________________
dense_2 (Dense)              (None, 2)                 102
=================================================================
Total params: 608
Trainable params: 608
Non-trainable params: 0
_________________________________________________________________
```

(Fig.8, AoA estimate using x,y location, path power, ToA, path loss and phase

A fourth simulation was conducted to test if, by using only path parameters, the AoA can be estimated accurately. The results are shown in Fig.9

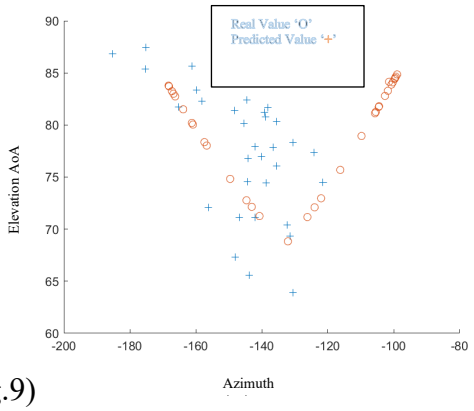

MAE: 15.850
MSE: 587.022, RMSE: 24.229
Model: "sequential"

Layer (type)	Output Shape	Param #
dense (Dense)	(None, 8)	40
dense_1 (Dense)	(None, 50)	450
dense_2 (Dense)	(None, 2)	102

Total params: 592
Trainable params: 592
Non-trainable params: 0

(Fig.9)

The second approach in testing the NN uses channel parameters as inputs in order to implement user localisation.

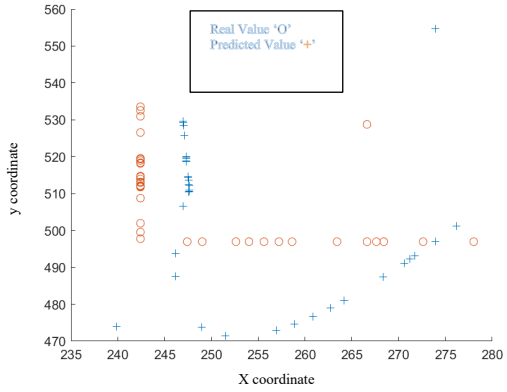


```
MAE: 5.865
MSE: 77.149, RMSE: 8.783
Model: "sequential"
_________________________________________________________________
Layer (type)                 Output Shape              Param #
=================================================================
dense (Dense)                (None, 8)                 24
_________________________________________________________________
dense_1 (Dense)              (None, 50)                450
_________________________________________________________________
dense_2 (Dense)              (None, 2)                 102
=================================================================
Total params: 576
Trainable params: 576
Non-trainable params: 0
_________________________________________________________________
```

(Fig.10, x,y location using only AoA)

- X,y based on AoA power and toa:

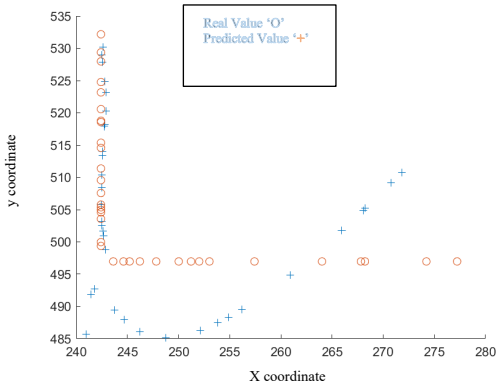


```
MAE: 2.975
MSE: 22.304, RMSE: 4.723
Model: "sequential"
_________________________________________________________________
Layer (type)                 Output Shape              Param #
=================================================================
dense (Dense)                (None, 8)                 40
_________________________________________________________________
dense_1 (Dense)              (None, 50)                450
_________________________________________________________________
dense_2 (Dense)              (None, 2)                 102
=================================================================
Total params: 592
Trainable params: 592
Non-trainable params: 0
_________________________________________________________________
```

(Fig.11, x,y location using only AoA, path power and ToA)

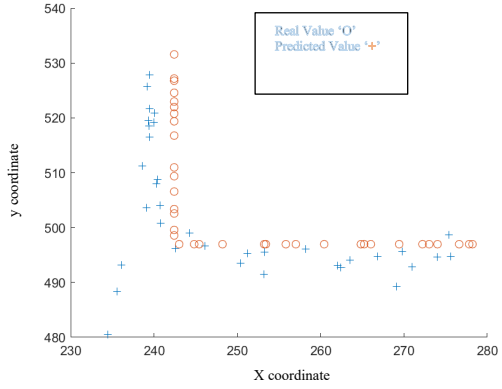


```
MAE: 3.321
MSE: 17.076, RMSE: 4.132
Model: "sequential"
_________________________________________________________________
Layer (type)                 Output Shape              Param #
=================================================================
dense (Dense)                (None, 8)                 56
_________________________________________________________________
dense_1 (Dense)              (None, 50)                450
_________________________________________________________________
dense_2 (Dense)              (None, 2)                 102
=================================================================
Total params: 608
Trainable params: 608
Non-trainable params: 0
_________________________________________________________________
```

(Fig.12, x,y location using only AoA, path power, path loss and phase)

5. DISCUSSION

Fig.6 shows a scatter plot that has the actual and predicted AoAs plotted on it. The only input for this simulation were the x and y coordinates of the user. This average RMSE for the dataset is 6.974 which shows an average tom poor performance by the NN. The greater magnitude of the RMSE value in comparison to the MAE value also shows that some, bigger than most, errors exist. The loss function is nowhere close to being minimized as its magnitude is 48.6This can also be seen in the on the scatter plot as some of the predicted values are far off from the actual values.

The results in Fig.7 show certain improvement. The loss function is significantly reduced and the MSE and RMSE values are closer to each other, this shows that average error between most of the predicted and actual values is small and somewhat equal to each other. This is also reflected in the scatter plot as many of the predicted and actual values are closer to each other. The improvements may be attributed to the two extra inputs, the path power and ToA. Having more inputs helps enables the NN to build a more accurate approximation function between the inputs and outputs.

The best results, for this approach, are displayed in Fig.8. The addition of two more parameters, the path phase and loss, show some improvement, even though not much. The loss function is nearly minimised; the values of MAE and RMSE are nearly 0 and quite close to each other. Many of the predicted and real values overlap on the scatter plot.

The outputs from the NN, even though they are close to convergence, do not fully converge. This can be seen as an issue, as the purpose of this NN is to be integrated into a beamformer, so it could help maintain a connection with a UE by estimating the AoA and feeding it to the beamformer so it knows where the next optimal channel vector would be. The work in [4] suggests that after a certain threshold for the AoA the UE disconnects. Hence, estimations must have minimal error.

An extra simulation is conducted in order to observe if the NN is able to predict accurate values of the AoA. This is not the case; the results are displayed in Fig.9. The NN does not learn how to estimate the AoA. This may be attributed to the fact that the raw channel parameters in themselves are closely linked, i.e., if one value goes up or down the other parameters will be, for every channel, effected in a direct or inverse manner.

For the second approach the raw channel parameters are input three different times in three different pairs. All three results are generally disappointing with the approach that takes all the generated channel parameters (AoA, path power, loss, phase and ToA), performing slightly better. The better performance of the NN when all channel parameters are used suggests that adding more inputs would help the NN build a better approximation function between inputs and outputs.

The most probable cause for the issues faced in user localisation could the methodology used to choose the hyper parameters. Several optimisers, activation functions and no. of nodes were trailed based upon similar simulation setups [4],[6] and [20]. This approach might provide near desirable results for one task, but that success does not translate to other tasks. The basic objective of the project, which are, to acquire a dataset that generates mmWave channels between BSs and UE, then leverage an ML model to estimate the AoA and implement user localisation is fulfilled. However, to suggest that the design is, in any way feasible to be integrated into a beamformer is incorrect nor should the simulations be deemed unsuccessful . The ML needs to be thoroughly optimised to fulfil the desired task properly.

6. CONCLUSION

The work done in this report proposes a design for a simple feedforward neural network that may be integrated into a beamformer to lessen the huge overhead that traditional beamformer require in order to form the optimal channel vectors. The solution to this problem is presented by producing a dataset that generates accurate mmWave channels between BSs and UE. The dataset is produced using the DeepMIMO dataset generator. An outdoor, main street scenario is considered. The data for 181 users with varying x and y locations is collected and raw channel parameters are fed as different sets of inputs in order to (i) estimate the AoA and (ii) using a different set of inputs, estimate the location of the user on the grid. The results show that the NN performs well with the AoA estimation approach, however, due to certain design limitations does not perform very well in user localisation.

Recommendations: Being able to identify certain flaws in my design. I would provide like to provide few suggestions for future work. Foremost would be use of Automated optimisers that only require the dataset, with the input features and output labels defined, which they then utilise to perform several combinations of activation functions, no. of layers and learning rates to find the optimal combinations. This methodology, applied by [20] and [4] would produce much better results.

Other than that, looking back at my results, the user localisation approach suggests that using more inputs aid in building a better approximation for the NN in order to make more accurate estimations.

BIBLIOGRAPHY

[1] 2022. Erricson Mobility Report. [online] Available at: <https://www.ericsson.com/en> [Accessed 10 May 2022].

[2] Jagannath, J., Polosky, N., Jagannath, A., Restuccia, F. and Melodia, T., 2019. Machine learning for wireless communications in the Internet of Things: A comprehensive survey. Ad Hoc Networks, 93, p.101913.

[3] Burghal, D., Abbasi, N.A. and Molisch, A.F., 2019, November. A machine learning solution for beam tracking in mmWave systems. In 2019 53rd Asilomar Conference on Signals, Systems, and Computers (pp. 173-177). IEEE.

[4] A Machine Learning Solution for Beam Tracking in mmWave Systems (2022). Available at: https://ieeexplore.ieee.org/document/9048770 (Accessed: 10 May 2022).

[5] F. Hussain, S. A. Hassan, R. Hussain and E. Hossain, "Machine Learning for Resource Management in Cellular and IoT Networks: Potentials, Current Solutions, and Open Challenges," in IEEE Communications Surveys & Tutorials, vol. 22, no. 2, pp. 1251-1275, Secondquarter 2020, doi: 10.1109/COMST.2020.2964534.

[5] B. M. ElHalawany, S. Hashima, K. Hatano, K. Wu and E. M. Mohamed, "Leveraging Machine Learning for Millimeter Wave Beamforming in Beyond 5G Networks," in IEEE Systems Journal, doi: 10.1109/JSYST.2021.3089536.

[6] Alkhateeb, A., Alex, S., Varkey, P., Li, Y., Qu, Q. and Tujkovic, D., 2018. Deep Learning Coordinated Beamforming for Highly-Mobile Millimeter Wave Systems. IEEE Access, 6, pp.37328-37348.

[7] Rappaport, T., Xing, Y., MacCartney, G., Molisch, A., Mellios, E. and Zhang, J., 2017. Overview of Millimeter Wave Communications for Fifth-Generation (5G) Wireless Networks—With a Focus on Propagation Models. IEEE Transactions on Antennas and Propagation, 65(12), pp.6213-6230.

[8] M. E. Morocho-Cayamcela, H. Lee and W. Lim, "Machine Learning for 5G/B5G Mobile and Wireless Communications: Potential, Limitations, and Future Directions," in IEEE Access, vol. 7, pp. 137184-137206, 2019, doi: 10.1109/ACCESS.2019.2942390.

[9] T. S. Rappaport et al., “Millimeter wave mobile communications for 5G cellular: It will work!” IEEE Access, vol. 1, pp. 335–349, May 2013.

[10] S. Rangan, T. S. Rappaport, and E. Erkip, “Millimeter-wave cellular wireless networks: Potentials and challenges,” Proc. IEEE, vol. 102, no. 3, pp. 366–385, Mar. 2014.

[11] A. Ghosh et al., “Millimeter-wave enhanced local area systems: A high-

data-rate approach for future wireless networks,” IEEE J. Sel. Areas Commun., vol. 32, no. 6, pp. 1152–1163, Jun. 2014.

[12] W. Roh et al., “Millimeter-wave beamforming as an enabling tech- nology for 5G cellular communications: Theoretical feasibility and prototype results,” IEEE Commun. Mag., vol. 52, no. 2, pp. 106–113, Feb. 2014

[13] S. G. Larew and D. J. Love, "Adaptive Beam Tracking With the Unscented Kalman Filter for Millimeter Wave Communication," in IEEE Signal Processing Letters, vol. 26, no. 11, pp. 1658-1662, Nov. 2019, doi: 10.1109/LSP.2019.2944255.

[14] S.Hur,T.Kim,D.J.Love,J.V.Krogmeier,T.A.Thomas,andA.Ghosh, ‘‘Millimeter wave beamforming for wireless backhaul and access in small cell networks,’’ IEEE Trans. Commun., vol. 61, no. 10, pp. 4391–4403, Oct. 2013.

[15] Goodfellow, I., Bengio, Y. and Courville, A., n.d. Deep learning.

[16] Ayodele, T.O. (2010) Introduction to Machine Learning. sine loco: IntechOpen.

[17] Hussain, F., Hassan, S., Hussain, R. and Hossain, E., 2020. Machine Learning for Resource Management in Cellular and IoT Networks: Potentials, Current Solutions, and Open Challenges. IEEE Communications Surveys & Tutorials, 22(2), pp.1251-1275.

[18] Deepmimo.net. 2022. DeepMIMO. [online] Available at: <https://deepmimo.net> [Accessed 10 May 2022].

[19] A.H.Carles and M.Xavire ‘Machine and Deep Learning-based Beam Selection for Hybrid Beamforming with Partial CSI’

[20] Bhattacherjee, U., Anjinappa, C.K., Smith, L., Ozturk, E. and Guvenc, I., 2020, March. Localization with deep neural networks using mmwave ray tracing simulations. In 2020 SoutheastCon (pp. 1-8). IEEE.

[21] Quadriga-channel-model.de. 2022. QuaDRiGa. [online] Available at: <https://quadriga-channel-model.de> [Accessed 10 May 2022].

[22] Mumtaz, S., Rodriguez, J. and Dai, L., 2017. MmWave massive MIMO. London, United Kingdom: Academic Press is an imprint of Elsevier.

[23] S. Aljumaily, M. and Li, H., 2020. Mobility Speed Effect and Neural Network Optimization for Deep MIMO Beamforming in mmWave Networks. International journal of Computer Networks & Communications, 12(6), pp.1-14.

[24] Remcom. 2022. Wireless EM Propagation Software - Wireless InSite — Remcom. [online] Available at: <https://www.remcom.com/wireless-insite-em-propagation-software> [Accessed 10 May 2022].

[25] Alkhateeb, A., 2022. DeepMIMO: A Generic Deep Learning Dataset for Millimeter Wave and Massive MIMO Applications. [online] arXiv.org. Available at: <https://arxiv.org/abs/1902.06435> [Accessed 10 May 2022].

[26] Medium. 2022. Understanding the 3 most common loss functions for Machine Learning Regression. [online] Available at: <https://towardsdatascience.com/understanding-the-3-most-common-loss-functions-for-machine-learning-regression-23e0ef3e14d3> [Accessed 10 May 2022].

[27] Team, K., 2022. Keras documentation: About Keras. [online] Keras.io. Available at: <https://keras.io/about/> [Accessed 10 May 2022].

APPENDIX

Chapter 3

3.2.2. The Neural Netwrok Architecture

NN_RG_MO.py

```python
from numpy import sqrt
import pandas as pd
from pandas import read_excel
from sklearn.metrics import mean_absolute_error
from sklearn.model_selection import train_test_split
from tensorflow.keras import Sequential
from tensorflow.keras.layers import Dense
from matplotlib import pyplot


# load the dataset
path = 'C:/Users/mc806/OneDrive - University of Sussex/Desktop/individual project/mmWave/dataset_1_path_loc.xls'
#path = 'C:/Users/mc806/OneDrive - University of Sussex/Desktop/individual project/mmWave/dataset_1_path_AoA.xls'
df = read_excel(path, header=-1)
print(df)
X, y = [df.values[:, 0:2], df.values[:, 2:4]]
print(X.shape, y.shape)

##model definition
X_train, X_test, y_train, y_test = train_test_split(X, y, test_size=0.10)
#print(X_train.shape, X_test.shape, y_train.shape, y_test.shape)
######

# determine the number of input features
n_features = X_train.shape[1]

# define model
model = Sequential()
model.add(Dense(8, activation='relu', kernel_initializer='he_normal', input_shape=(n_features,)))
model.add(Dense(50, activation='relu', kernel_initializer='he_normal'))
model.add(Dense(2))

# compile the model
model.compile(optimizer='adam', loss='mse')

from tensorflow.keras.optimizers import Adam
# fit the model
model.fit(X_train, y_train, epochs=350, batch_size=1, verbose=2)
# evaluate the model
error = model.evaluate(X_test, y_test, verbose=2)



##prediction
yhat = model.predict([X_test])
print(yhat)
print(X_test)
data = pd.DataFrame(yhat)
datatoexcel = pd.ExcelWriter("C:/Users/mc806/OneDrive - University of Sussex/Desktop/individual project/mmWave/prediction_1.xlsx", engine="openpyxl")
data.to_excel(datatoexcel, sheet_name='Sheet1')
datatoexcel.save()
data2 = pd.DataFrame(y_test)
datatoexcel = pd.ExcelWriter("C:/Users/mc806/OneDrive - University of Sussex/Desktop/individual project/mmWave/ACTUAL_1.xlsx", engine="openpyxl")
data2.to_excel(datatoexcel, sheet_name='Sheet1')
datatoexcel.save()
mae = mean_absolute_error(y_test, yhat)
print('MAE: %.3f' % mae)
print('MSE: %.3f, RMSE: %.3f' % (error, sqrt(error)))
```

```python
##model sumarry#
model.summary()
history = model.fit(X, y, epochs=350, batch_size=1, verbose=0, validation_split=0.15)
pyplot.title('Learning Curves')
pyplot.xlabel('Epoch')
pyplot.ylabel('Cross Entropy')
pyplot.plot(history.history['loss'], label='train')
pyplot.plot(history.history['val_loss'], label='val')
pyplot.legend()
pyplot.show()
```

Dataset for AoA pereddiction:

x	y	phase	ToA	Power	pathloss	AoA	AoA
242.423	496.9710083	86.2506	3.65E-08	1.27E-09	10.9377	-132.818	68.5488
242.623	496.9710083	-110.454	3.69E-08	1.24E-09	11.0653	-133.633	68.8082
242.823	496.9710083	-99.8663	3.74E-08	1.22E-09	11.195	-134.426	69.0654
243.023	496.9710083	123.26	3.78E-08	1.19E-09	11.3268	-135.198	69.3202
243.223	496.9710083	-155.988	3.82E-08	1.16E-09	11.4605	-135.95	69.5724
243.423	496.9710083	147.314	3.87E-08	1.13E-09	11.5962	-136.682	69.8218
243.623	496.9710083	-42.0646	3.92E-08	1.1E-09	11.7337	-137.395	70.0683
243.823	496.9710083	0.484133	3.96E-08	1.08E-09	11.8729	-138.089	70.3118
244.023	496.9710083	-80.5856	4.01E-08	1.05E-09	12.0139	-138.765	70.5522
244.223	496.9710083	79.0272	4.06E-08	1.03E-09	12.1566	-139.422	70.7894
244.423	496.9710083	123.473	4.1E-08	1E-09	12.3008	-140.063	71.0234
244.623	496.9710083	56.7563	4.15E-08	9.79E-10	12.4466	-140.687	71.254
244.823	496.9710083	-117.263	4.2E-08	9.56E-10	12.5938	-141.295	71.4812
245.023	496.9710083	-34.8655	4.25E-08	9.33E-10	12.7425	-141.888	71.705
245.223	496.9710083	-52.4657	4.3E-08	9.11E-10	12.8926	-142.465	71.9254
245.423	496.9710083	-166.612	4.35E-08	8.9E-10	13.0441	-143.027	72.1424
245.623	496.9710083	-13.9816	4.4E-08	8.69E-10	13.1968	-143.575	72.3559
245.823	496.9710083	48.6256	4.45E-08	8.49E-10	13.3508	-144.109	72.5659
246.023	496.9710083	24.2882	4.51E-08	8.29E-10	13.5059	-144.63	72.7725
246.223	496.9710083	-84.0312	4.56E-08	8.1E-10	13.6623	-145.138	72.9757
246.423	496.9710083	86.5178	4.61E-08	7.91E-10	13.8198	-145.633	73.1755
246.623	496.9710083	178.677	4.66E-08	7.73E-10	13.9783	-146.116	73.3719
246.823	496.9710083	-164.916	4.72E-08	7.55E-10	14.1379	-146.587	73.565
247.023	496.9710083	138.276	4.77E-08	7.38E-10	14.2986	-147.047	73.7548
247.223	496.9710083	10.6915	4.82E-08	7.21E-10	14.4602	-147.495	73.9413
247.423	496.9710083	174.678	4.88E-08	7.04E-10	14.6227	-147.933	74.1246
247.623	496.9710083	-87.5068	4.93E-08	6.89E-10	14.7862	-148.361	74.3046
247.823	496.9710083	-53.6935	4.99E-08	6.73E-10	14.9506	-148.778	74.4816
248.023	496.9710083	-81.7939	5.04E-08	6.58E-10	15.1158	-149.185	74.6554
248.223	496.9710083	-169.8	5.1E-08	6.44E-10	15.2818	-149.583	74.8261
248.423	496.9710083	44.2206	5.15E-08	6.29E-10	15.4487	-149.972	74.9939
248.623	496.9710083	-157.875	5.21E-08	6.16E-10	15.6163	-150.352	75.1587
248.823	496.9710083	-54.2972	5.27E-08	6.02E-10	15.7847	-150.723	75.3206
249.023	496.9710083	-3.3273	5.32E-08	5.89E-10	15.9538	-151.086	75.4797
249.223	496.9710083	-3.30932	5.38E-08	5.77E-10	16.1237	-151.441	75.6359
249.423	496.9710083	-52.6501	5.44E-08	5.64E-10	16.2942	-151.788	75.7894
249.623	496.9710083	-149.816	5.49E-08	5.52E-10	16.4654	-152.127	75.9402
249.823	496.9710083	66.6683	5.55E-08	5.41E-10	16.6372	-152.459	76.0883
250.023	496.9710083	-121.775	5.61E-08	5.29E-10	16.8096	-152.783	76.2339
250.223	496.9710083	6.2225	5.67E-08	5.18E-10	16.9827	-153.101	76.3769
250.423	496.9710083	91.9787	5.72E-08	5.08E-10	17.1563	-153.411	76.5174
250.623	496.9710083	136.763	5.78E-08	4.97E-10	17.3305	-153.716	76.6554
250.823	496.9710083	141.8	5.84E-08	4.87E-10	17.5052	-154.013	76.7911
251.023	496.9710083	108.266	5.9E-08	4.77E-10	17.6805	-154.305	76.9243
251.223	496.9710083	37.2983	5.96E-08	4.67E-10	17.8563	-154.59	77.0553
251.423	496.9710083	-70.0084	6.02E-08	4.58E-10	18.0327	-154.87	77.1841
251.623	496.9710083	147.401	6.08E-08	4.49E-10	18.2095	-155.144	77.3106
251.823	496.9710083	-29.4545	6.14E-08	4.4E-10	18.3867	-155.412	77.4349
252.023	496.9710083	120.406	6.19E-08	4.31E-10	18.5645	-155.675	77.5572
252.223	496.9710083	-122.072	6.25E-08	4.23E-10	18.7427	-155.933	77.6773
252.423	496.9710083	-35.9724	6.31E-08	4.15E-10	18.9213	-156.186	77.7955

252.623	496.9710083	19.5849	6.37E-08	4.07E-10	19.1003	-156.434	77.9116
252.823	496.9710083	45.4511	6.43E-08	3.99E-10	19.2798	-156.676	78.0258
253.023	496.9710083	42.4476	6.49E-08	3.92E-10	19.4596	-156.915	78.1381
253.223	496.9710083	11.3677	6.55E-08	3.84E-10	19.6399	-157.148	78.2485
253.423	496.9710083	-47.0227	6.61E-08	3.77E-10	19.8205	-157.378	78.3571
253.623	496.9710083	-131.984	6.67E-08	3.7E-10	20.0015	-157.603	78.4639
253.823	496.9710083	117.199	6.73E-08	3.63E-10	20.1829	-157.823	78.569
254.023	496.9710083	-18.7823	6.8E-08	3.56E-10	20.3646	-158.04	78.6723
254.223	496.9710083	-179.261	6.86E-08	3.5E-10	20.5466	-158.252	78.774
254.423	496.9710083	-3.59258	6.92E-08	3.44E-10	20.729	-158.461	78.874
254.623	496.9710083	148.848	6.98E-08	3.37E-10	20.9117	-158.666	78.9725
254.823	496.9710083	-81.3349	7.04E-08	3.31E-10	21.0947	-158.867	79.0693
255.023	496.9710083	26.4411	7.1E-08	3.26E-10	21.278	-159.065	79.1646
255.223	496.9710083	112.741	7.16E-08	3.2E-10	21.4616	-159.259	79.2584
255.423	496.9710083	178.112	7.22E-08	3.14E-10	21.6455	-159.45	79.3508
255.623	496.9710083	-136.917	7.28E-08	3.09E-10	21.8297	-159.638	79.4417
255.823	496.9710083	-111.835	7.35E-08	3.03E-10	22.0142	-159.822	79.5311
256.023	496.9710083	-106.145	7.41E-08	2.98E-10	22.1989	-160.003	79.6192
256.223	496.9710083	-119.367	7.47E-08	2.93E-10	22.3839	-160.181	79.706
256.423	496.9710083	-151.037	7.53E-08	2.88E-10	22.5692	-160.356	79.7914
256.623	496.9710083	159.296	7.59E-08	2.83E-10	22.7547	-160.528	79.8755
256.823	496.9710083	92.0698	7.65E-08	2.79E-10	22.9404	-160.697	79.9583
257.023	496.9710083	7.70613	7.72E-08	2.74E-10	23.1264	-160.863	80.0399
257.223	496.9710083	-93.3844	7.78E-08	2.69E-10	23.3126	-161.027	80.1202
257.423	496.9710083	149.196	7.84E-08	2.65E-10	23.4991	-161.187	80.1994
257.623	496.9710083	15.8323	7.9E-08	2.61E-10	23.6857	-161.346	80.2774
257.823	496.9710083	-133.101	7.97E-08	2.56E-10	23.8726	-161.501	80.3542
258.023	496.9710083	62.7593	8.03E-08	2.52E-10	24.0597	-161.655	80.43
258.223	496.9710083	-116.236	8.09E-08	2.48E-10	24.247	-161.806	80.5046
258.423	496.9710083	50.2565	8.15E-08	2.44E-10	24.4345	-161.954	80.5781
258.623	496.9710083	-157.433	8.22E-08	2.4E-10	24.6222	-162.1	80.6506
258.823	496.9710083	-18.9827	8.28E-08	2.37E-10	24.8101	-162.244	80.722
259.023	496.9710083	105.92	8.34E-08	2.33E-10	24.9981	-162.386	80.7924
259.223	496.9710083	-142.42	8.4E-08	2.29E-10	25.1864	-162.525	80.8618
259.423	496.9710083	-43.7098	8.47E-08	2.26E-10	25.3748	-162.662	80.9303
259.623	496.9710083	42.3378	8.53E-08	2.22E-10	25.5634	-162.798	80.9977
259.823	496.9710083	116.001	8.59E-08	2.19E-10	25.7522	-162.931	81.0643
260.023	496.9710083	177.55	8.66E-08	2.16E-10	25.9412	-163.062	81.1299
260.223	496.9710083	-132.752	8.72E-08	2.12E-10	26.1303	-163.191	81.1946
260.423	496.9710083	-94.6502	8.78E-08	2.09E-10	26.3196	-163.319	81.2584
260.623	496.9710083	-67.8956	8.85E-08	2.06E-10	26.509	-163.444	81.3214
260.823	496.9710083	-52.2469	8.91E-08	2.03E-10	26.6986	-163.568	81.3835
261.023	496.9710083	-47.4692	8.97E-08	2E-10	26.8883	-163.69	81.4447
261.223	496.9710083	-53.334	9.04E-08	1.97E-10	27.0782	-163.81	81.5052
261.423	496.9710083	-69.6188	9.1E-08	1.94E-10	27.2683	-163.928	81.5648
261.623	496.9710083	-96.1074	9.16E-08	1.92E-10	27.4584	-164.045	81.6236
261.823	496.9710083	-132.589	9.23E-08	1.89E-10	27.6488	-164.16	81.6817
262.023	496.9710083	-178.859	9.29E-08	1.86E-10	27.8392	-164.274	81.739
262.223	496.9710083	125.282	9.35E-08	1.84E-10	28.0298	-164.386	81.7956
262.423	496.9710083	60.0286	9.42E-08	1.81E-10	28.2205	-164.496	81.8514
262.623	496.9710083	-14.43	9.48E-08	1.78E-10	28.4113	-164.605	81.9065
262.823	496.9710083	-97.9096	9.54E-08	1.76E-10	28.6023	-164.713	81.9609
263.023	496.9710083	169.769	9.61E-08	1.73E-10	28.7934	-164.819	82.0146

263.223	496.9710083	68.7814	9.67E-08	1.71E-10	28.9846	-164.923	82.0676
263.423	496.9710083	-40.7027	9.74E-08	1.69E-10	29.1759	-165.026	82.12
263.623	496.9710083	-158.517	9.8E-08	1.66E-10	29.3674	-165.128	82.1717
263.823	496.9710083	75.5002	9.86E-08	1.64E-10	29.5589	-165.228	82.2227
264.023	496.9710083	-58.4931	9.93E-08	1.62E-10	29.7506	-165.327	82.2731
264.223	496.9710083	159.657	9.99E-08	1.6E-10	29.9424	-165.425	82.3229
264.423	496.9710083	10.1001	1.01E-07	1.58E-10	30.1342	-165.522	82.3721
264.623	496.9710083	-147.017	1.01E-07	1.56E-10	30.3262	-165.617	82.4207
264.823	496.9710083	48.4478	1.02E-07	1.54E-10	30.5183	-165.711	82.4686
265.023	496.9710083	-123.366	1.02E-07	1.52E-10	30.7105	-165.804	82.516
265.223	496.9710083	57.6777	1.03E-07	1.5E-10	30.9028	-165.896	82.5629
265.423	496.9710083	-128.289	1.04E-07	1.48E-10	31.0952	-165.986	82.6091
265.623	496.9710083	38.8634	1.04E-07	1.46E-10	31.2877	-166.076	82.6549
265.823	496.9710083	-160.739	1.05E-07	1.44E-10	31.4802	-166.164	82.7
266.023	496.9710083	-6.97294	1.06E-07	1.42E-10	31.6729	-166.251	82.7447
266.223	496.9710083	140.282	1.06E-07	1.4E-10	31.8657	-166.337	82.7888
266.423	496.9710083	-78.857	1.07E-07	1.38E-10	32.0585	-166.423	82.8324
266.623	496.9710083	55.7249	1.08E-07	1.37E-10	32.2515	-166.507	82.8755
266.823	496.9710083	-175.86	1.08E-07	1.35E-10	32.4445	-166.59	82.9181
267.023	496.9710083	-53.503	1.09E-07	1.33E-10	32.6376	-166.672	82.9602
267.223	496.9710083	62.9035	1.1E-07	1.32E-10	32.8308	-166.753	83.0019
267.423	496.9710083	173.464	1.1E-07	1.3E-10	33.024	-166.833	83.043
267.623	496.9710083	-81.7206	1.11E-07	1.28E-10	33.2174	-166.912	83.0837
267.823	496.9710083	17.4507	1.11E-07	1.27E-10	33.4108	-166.99	83.124
268.023	496.9710083	111.075	1.12E-07	1.25E-10	33.6043	-167.068	83.1637
268.223	496.9710083	-160.753	1.13E-07	1.24E-10	33.7979	-167.144	83.2031
268.423	496.9710083	-77.9391	1.13E-07	1.22E-10	33.9915	-167.22	83.242
268.623	496.9710083	-0.39297	1.14E-07	1.21E-10	34.1853	-167.294	83.2805
268.823	496.9710083	71.9746	1.15E-07	1.19E-10	34.3791	-167.368	83.3185
269.023	496.9710083	139.251	1.15E-07	1.18E-10	34.5729	-167.441	83.3561
269.223	496.9710083	-158.48	1.16E-07	1.17E-10	34.7669	-167.513	83.3934
269.423	496.9710083	-101.133	1.17E-07	1.15E-10	34.9609	-167.584	83.4302
269.623	496.9710083	-48.6275	1.17E-07	1.14E-10	35.155	-167.655	83.4666
269.823	496.9710083	-0.88397	1.18E-07	1.13E-10	35.3491	-167.725	83.5027
270.023	496.9710083	42.1759	1.19E-07	1.11E-10	35.5433	-167.794	83.5383
270.223	496.9710083	80.6284	1.19E-07	1.1E-10	35.7376	-167.862	83.5736
270.423	496.9710083	114.548	1.2E-07	1.09E-10	35.9319	-167.929	83.6085
270.623	496.9710083	144.009	1.21E-07	1.08E-10	36.1263	-167.996	83.643
270.823	496.9710083	169.081	1.21E-07	1.06E-10	36.3207	-168.062	83.6772
271.023	496.9710083	-170.164	1.22E-07	1.05E-10	36.5153	-168.128	83.711
271.223	496.9710083	-153.658	1.22E-07	1.04E-10	36.7098	-168.192	83.7445
271.423	496.9710083	-141.335	1.23E-07	1.03E-10	36.9045	-168.256	83.7776
271.623	496.9710083	-133.127	1.24E-07	1.02E-10	37.0992	-168.319	83.8104
271.823	496.9710083	-128.971	1.24E-07	1.01E-10	37.2939	-168.382	83.8428
272.023	496.9710083	-128.804	1.25E-07	9.95E-11	37.4887	-168.444	83.8749
272.223	496.9710083	-132.563	1.26E-07	9.84E-11	37.6836	-168.505	83.9067
272.423	496.9710083	-140.188	1.26E-07	9.73E-11	37.8785	-168.566	83.9382
272.623	496.9710083	-151.62	1.27E-07	9.63E-11	38.0734	-168.626	83.9694
272.823	496.9710083	-166.801	1.28E-07	9.52E-11	38.2684	-168.685	84.0002
273.023	496.9710083	174.327	1.28E-07	9.42E-11	38.4635	-168.744	84.0308
273.223	496.9710083	151.82	1.29E-07	9.32E-11	38.6586	-168.802	84.061
273.423	496.9710083	125.731	1.3E-07	9.22E-11	38.8538	-168.86	84.0909
273.623	496.9710083	96.1156	1.3E-07	9.12E-11	39.049	-168.917	84.1206

273.823	496.9710083	63.0256	1.31E-07	9.03E-11	39.2443	-168.973	84.1499
274.023	496.9710083	26.5126	1.32E-07	8.93E-11	39.4396	-169.029	84.179
274.223	496.9710083	-13.3726	1.32E-07	8.84E-11	39.6349	-169.084	84.2078
274.423	496.9710083	-56.5806	1.33E-07	8.75E-11	39.8303	-169.139	84.2363
274.623	496.9710083	-103.063	1.34E-07	8.65E-11	40.0258	-169.193	84.2645
274.823	496.9710083	-152.771	1.34E-07	8.56E-11	40.2213	-169.247	84.2925
275.023	496.9710083	154.341	1.35E-07	8.48E-11	40.4168	-169.3	84.3202
275.223	496.9710083	98.3202	1.36E-07	8.39E-11	40.6124	-169.353	84.3477
275.423	496.9710083	39.2104	1.36E-07	8.3E-11	40.808	-169.405	84.3748
275.623	496.9710083	-22.9436	1.37E-07	8.22E-11	41.0037	-169.456	84.4018
275.823	496.9710083	-88.0986	1.37E-07	8.14E-11	41.1994	-169.508	84.4284
276.023	496.9710083	-156.212	1.38E-07	8.06E-11	41.3951	-169.558	84.4549
276.223	496.9710083	132.758	1.39E-07	7.97E-11	41.5909	-169.608	84.4811
276.423	496.9710083	58.8526	1.39E-07	7.9E-11	41.7867	-169.658	84.507
276.623	496.9710083	-17.8882	1.4E-07	7.82E-11	41.9826	-169.707	84.5327
276.823	496.9710083	-97.4249	1.41E-07	7.74E-11	42.1785	-169.756	84.5582
277.023	496.9710083	-179.719	1.41E-07	7.66E-11	42.3744	-169.804	84.5834
277.223	496.9710083	95.2685	1.42E-07	7.59E-11	42.5704	-169.852	84.6084
277.423	496.9710083	7.57411	1.43E-07	7.51E-11	42.7664	-169.9	84.6332
277.623	496.9710083	-82.7652	1.43E-07	7.44E-11	42.9625	-169.947	84.6578
277.823	496.9710083	-175.713	1.44E-07	7.37E-11	43.1586	-169.993	84.6821
278.023	496.9710083	88.765	1.45E-07	7.3E-11	43.3547	-170.039	84.7062
278.223	496.9710083	-9.29539	1.45E-07	7.23E-11	43.5509	-170.085	84.7302
278.423	496.9710083	-109.86	1.46E-07	7.16E-11	43.7471	-170.13	84.7539
242.423	497.17099	-104.189	3.7E-08	1.24E-09	11.0752	-132.064	68.8281
242.423	497.3710022	-70.1938	3.74E-08	1.21E-09	11.2146	-131.331	69.1036
242.423	497.5710144	-166.773	3.79E-08	1.18E-09	11.3558	-130.619	69.3754
242.423	497.7709961	-29.1161	3.84E-08	1.15E-09	11.4987	-129.927	69.6432
242.423	497.9710083	-12.5912	3.89E-08	1.12E-09	11.6433	-129.254	69.9071
242.423	498.17099	-112.74	3.93E-08	1.09E-09	11.7896	-128.601	70.1668
266.623	498.17099	121.846	1.09E-07	1.34E-10	32.5502	-164.437	82.9413
242.423	498.5710144	73.9255	4.03E-08	1.04E-09	12.0867	-127.347	70.674
242.823	498.7709961	-45.9798	4.16E-08	9.76E-10	12.468	-128.301	71.2874
242.423	498.9710083	-156.766	4.13E-08	9.88E-10	12.3896	-126.161	71.1645
242.423	499.17099	-59.1956	4.19E-08	9.64E-10	12.5431	-125.592	71.4035
242.423	499.3710022	-54.9496	4.24E-08	9.4E-10	12.6979	-125.039	71.6384
242.423	499.5710144	-140.657	4.29E-08	9.17E-10	12.8539	-124.5	71.8691
242.423	499.7709961	46.9181	4.34E-08	8.94E-10	13.0111	-123.976	72.0956
242.423	499.9710083	150.882	4.39E-08	8.73E-10	13.1695	-123.466	72.3181
242.423	500.17099	174.216	4.45E-08	8.51E-10	13.329	-122.969	72.5366
242.423	500.3710022	119.779	4.5E-08	8.31E-10	13.4896	-122.485	72.7511
242.423	500.5710144	-9.68322	4.56E-08	8.11E-10	13.6513	-122.013	72.9616
242.423	500.7709961	148.463	4.61E-08	7.91E-10	13.8139	-121.554	73.1682
242.423	500.9710083	-123.256	4.66E-08	7.73E-10	13.9775	-121.106	73.371
242.423	501.17099	-102.415	4.72E-08	7.54E-10	14.1421	-120.669	73.57
242.423	501.3710022	-146.688	4.77E-08	7.37E-10	14.3075	-120.244	73.7652
242.423	501.5710144	106.159	4.83E-08	7.19E-10	14.4738	-119.829	73.9569
242.423	501.7709961	-61.7314	4.89E-08	7.03E-10	14.641	-119.424	74.1449
242.423	501.9710083	71.6973	4.94E-08	6.86E-10	14.809	-119.029	74.3294
242.423	502.17099	148.42	5E-08	6.71E-10	14.9777	-118.644	74.5104
242.423	502.3710022	170.331	5.05E-08	6.55E-10	15.1472	-118.268	74.688
242.423	502.5710144	139.251	5.11E-08	6.41E-10	15.3175	-117.901	74.8623
242.423	502.7709961	56.9272	5.17E-08	6.26E-10	15.4885	-117.543	75.0334

242.423	502.9710083	-74.9618	5.23E-08	6.12E-10	15.6601	-117.193	75.2012
242.423	502.9710083	-74.9618	5.23E-08	6.12E-10	15.6601	-117.193	75.2012
242.423	503.17099	105.196	5.28E-08	5.99E-10	15.8325	-116.851	75.3659
242.423	503.3710022	-121.05	5.34E-08	5.85E-10	16.0054	-116.517	75.5275
242.423	503.3710022	-121.05	5.34E-08	5.85E-10	16.0054	-116.517	75.5275
242.423	503.5710144	-32.2128	5.4E-08	5.73E-10	16.179	-116.191	75.6861
242.423	503.7709961	13.1392	5.46E-08	5.6E-10	16.3532	-115.872	75.8418
277.423	503.7709961	-70.1522	1.48E-07	6.91E-11	44.4608	-161.204	84.8383
242.423	504.17099	-21.1671	5.57E-08	5.36E-10	16.7033	-115.255	76.1445
242.423	504.3710022	-98.2324	5.63E-08	5.25E-10	16.8792	-114.957	76.2918
242.423	504.5710144	146.407	5.69E-08	5.14E-10	17.0556	-114.665	76.4363
242.423	504.7709961	-6.07178	5.75E-08	5.03E-10	17.2326	-114.38	76.5782
242.423	504.9710083	165.462	5.81E-08	4.92E-10	17.41	-114.101	76.7175
242.423	505.17099	-57.9024	5.87E-08	4.82E-10	17.5879	-113.828	76.8543
242.423	505.3710022	44.8838	5.93E-08	4.72E-10	17.7663	-113.56	76.9886
242.423	505.5710144	114.83	5.99E-08	4.63E-10	17.9452	-113.298	77.1205
242.423	505.7709961	152.908	6.05E-08	4.53E-10	18.1245	-113.042	77.2501
242.423	505.9710083	160.055	6.11E-08	4.44E-10	18.3042	-112.791	77.3773
242.423	506.17099	137.173	6.17E-08	4.35E-10	18.4843	-112.545	77.5023
242.423	506.3710022	85.1304	6.23E-08	4.27E-10	18.6649	-112.304	77.6252
242.423	506.5710144	4.76641	6.29E-08	4.18E-10	18.8458	-112.068	77.7458
242.423	506.7709961	-103.111	6.35E-08	4.1E-10	19.0271	-111.836	77.8644
242.423	506.9710083	122.276	6.41E-08	4.02E-10	19.2088	-111.609	77.9809
242.423	507.17099	-38.3194	6.47E-08	3.94E-10	19.3908	-111.387	78.0954
242.423	507.3710022	135.827	6.53E-08	3.87E-10	19.5732	-111.169	78.2079
242.423	507.5710144	-74.5857	6.59E-08	3.8E-10	19.756	-110.955	78.3185
242.423	507.7709961	51.1184	6.65E-08	3.72E-10	19.939	-110.745	78.4273
277.423	507.7709961	171.124	1.53E-07	6.46E-11	45.901	-156.454	85.0007
242.423	508.17099	-126.539	6.78E-08	3.59E-10	20.3061	-110.337	78.6393
242.423	508.3710022	-68.6623	6.84E-08	3.52E-10	20.4901	-110.139	78.7427
242.423	508.5710144	-32.1929	6.9E-08	3.46E-10	20.6744	-109.945	78.8443
242.423	508.7709961	-16.5631	6.96E-08	3.39E-10	20.859	-109.754	78.9443
242.423	508.9710083	-21.2243	7.02E-08	3.33E-10	21.0439	-109.566	79.0426
242.423	509.17099	-45.6465	7.08E-08	3.27E-10	21.2291	-109.382	79.1394
242.423	509.3710022	-89.3171	7.15E-08	3.21E-10	21.4145	-109.201	79.2345
242.423	509.5710144	-151.74	7.21E-08	3.16E-10	21.6002	-109.024	79.3282
242.423	509.7709961	127.563	7.27E-08	3.1E-10	21.7861	-108.85	79.4203
277.423	509.7709961	-31.7422	1.56E-07	6.21E-11	46.733	-154.197	85.0899
242.423	510.17099	-86.8092	7.39E-08	2.99E-10	22.1587	-108.51	79.6002
242.423	510.3710022	140.399	7.46E-08	2.94E-10	22.3453	-108.344	79.688
242.423	510.5710144	-8.89895	7.52E-08	2.89E-10	22.5322	-108.182	79.7745
242.423	510.7709961	-174.294	7.58E-08	2.84E-10	22.7193	-108.022	79.8596
242.423	510.9710083	4.60646	7.64E-08	2.79E-10	22.9067	-107.865	79.9434
242.423	511.17099	168.186	7.71E-08	2.75E-10	23.0942	-107.71	80.0259
242.423	511.3710022	-43.1856	7.77E-08	2.7E-10	23.2819	-107.558	80.1071
242.423	511.5710144	90.8505	7.83E-08	2.66E-10	23.4699	-107.409	80.1871
242.423	511.7709961	-149.358	7.89E-08	2.61E-10	23.658	-107.262	80.2659
242.423	511.9710083	-43.4738	7.96E-08	2.57E-10	23.8464	-107.117	80.3435
242.423	512.1710205	48.8298	8.02E-08	2.53E-10	24.0349	-106.975	80.42
242.423	512.3709717	127.87	8.08E-08	2.49E-10	24.2236	-106.835	80.4953
242.423	512.5709839	-166.045	8.15E-08	2.45E-10	24.4125	-106.697	80.5695
242.423	512.7709961	-112.618	8.21E-08	2.41E-10	24.6016	-106.561	80.6427
242.423	512.9710083	-71.5591	8.27E-08	2.37E-10	24.7908	-106.428	80.7147

242.423	513.1710205	-42.5865	8.34E-08	2.33E-10	24.9802	-106.296	80.7857
242.423	513.3709717	-25.4277	8.4E-08	2.3E-10	25.1698	-106.167	80.8557
242.423	513.5709839	-19.8179	8.46E-08	2.26E-10	25.3595	-106.039	80.9247
242.423	513.7709961	-25.4997	8.53E-08	2.23E-10	25.5494	-105.914	80.9927
242.423	513.9710083	-42.2232	8.59E-08	2.19E-10	25.7394	-105.79	81.0598
242.423	514.1710205	-69.7457	8.65E-08	2.16E-10	25.9296	-105.669	81.1259
242.423	514.3709717	-107.831	8.72E-08	2.13E-10	26.12	-105.549	81.1911
242.423	514.5709839	-156.251	8.78E-08	2.09E-10	26.3104	-105.431	81.2554
242.423	514.7709961	145.219	8.84E-08	2.06E-10	26.5011	-105.314	81.3187
242.423	514.9710083	76.7945	8.91E-08	2.03E-10	26.6918	-105.2	81.3813
242.423	515.1710205	-1.31391	8.97E-08	2E-10	26.8827	-105.087	81.4429
242.423	515.3709717	-88.9012	9.03E-08	1.97E-10	27.0737	-104.975	81.5037
242.423	515.5709839	174.232	9.1E-08	1.94E-10	27.2649	-104.865	81.5638
242.423	515.7709961	68.279	9.16E-08	1.92E-10	27.4562	-104.757	81.6229
242.423	515.9710083	-46.5711	9.23E-08	1.89E-10	27.6476	-104.65	81.6814
242.423	516.1710205	-170.135	9.29E-08	1.86E-10	27.8391	-104.545	81.739
242.423	516.3709717	57.766	9.35E-08	1.84E-10	28.0307	-104.442	81.7959
242.423	516.5709839	-82.6943	9.42E-08	1.81E-10	28.2225	-104.339	81.852
242.423	516.7709961	128.653	9.48E-08	1.78E-10	28.4143	-104.238	81.9074
242.423	516.9710083	-28.026	9.55E-08	1.76E-10	28.6063	-104.139	81.962
242.423	517.1710205	167.428	9.61E-08	1.73E-10	28.7984	-104.041	82.016
242.423	517.3709717	-4.82835	9.67E-08	1.71E-10	28.9906	-103.944	82.0693
242.423	517.5709839	175.357	9.74E-08	1.69E-10	29.1829	-103.848	82.1219
242.423	517.7709961	-11.8663	9.8E-08	1.66E-10	29.3753	-103.754	82.1738
242.423	517.9710083	153.645	9.87E-08	1.64E-10	29.5678	-103.661	82.2251
242.423	518.1710205	-47.9673	9.93E-08	1.62E-10	29.7604	-103.569	82.2757
242.423	518.3709717	103.434	9.99E-08	1.6E-10	29.9531	-103.479	82.3257
242.423	518.5709839	-112.017	1.01E-07	1.58E-10	30.1459	-103.389	82.3751
242.423	518.7709961	25.8095	1.01E-07	1.55E-10	30.3388	-103.301	82.4238
242.423	518.9710083	157.042	1.02E-07	1.53E-10	30.5318	-103.214	82.472
242.423	519.1710205	-78.1958	1.03E-07	1.51E-10	30.7249	-103.128	82.5196
242.423	519.3709717	40.2175	1.03E-07	1.49E-10	30.918	-103.043	82.5666
242.423	519.5709839	152.4	1.04E-07	1.47E-10	31.1113	-102.959	82.613
242.423	519.7709961	-101.533	1.04E-07	1.46E-10	31.3046	-102.877	82.6589
277.423	519.7709961	-92.4635	1.73E-07	4.96E-11	51.8586	-144.169	85.5762
242.423	520.1710205	92.7039	1.06E-07	1.42E-10	31.6915	-102.714	82.749
242.423	520.3709717	-178.91	1.06E-07	1.4E-10	31.8851	-102.634	82.7932
242.423	520.5709839	-96.2043	1.07E-07	1.38E-10	32.0787	-102.556	82.837
242.423	520.7709961	-19.0773	1.08E-07	1.37E-10	32.2725	-102.478	82.8802
242.423	520.9710083	52.571	1.08E-07	1.35E-10	32.4663	-102.401	82.9229
242.423	521.1710205	118.838	1.09E-07	1.33E-10	32.6602	-102.325	82.9651
242.423	521.3709717	179.82	1.1E-07	1.31E-10	32.8541	-102.25	83.0069
242.423	521.5709839	-124.392	1.1E-07	1.3E-10	33.0482	-102.176	83.0481
242.423	521.7709961	-73.7051	1.11E-07	1.28E-10	33.2422	-102.103	83.0889
242.423	521.9710083	-28.0314	1.12E-07	1.27E-10	33.4364	-102.03	83.1292
242.423	522.1710205	12.7161	1.12E-07	1.25E-10	33.6307	-101.959	83.1691
242.423	522.3709717	48.6223	1.13E-07	1.24E-10	33.825	-101.888	83.2085
242.423	522.5709839	79.7701	1.14E-07	1.22E-10	34.0193	-101.818	83.2475
242.423	522.7709961	106.241	1.14E-07	1.21E-10	34.2138	-101.749	83.2861
242.423	522.9710083	128.113	1.15E-07	1.19E-10	34.4083	-101.681	83.3242
242.423	523.1710205	145.465	1.15E-07	1.18E-10	34.6028	-101.613	83.3619
242.423	523.3709717	158.373	1.16E-07	1.16E-10	34.7974	-101.547	83.3992
242.423	523.5709839	166.91	1.17E-07	1.15E-10	34.9921	-101.481	83.4361

242.423	523.7709961	171.149	1.17E-07	1.14E-10	35.1869	-101.415	83.4726
242.423	523.9710083	171.161	1.18E-07	1.12E-10	35.3817	-101.351	83.5087
242.423	524.1710205	167.016	1.19E-07	1.11E-10	35.5765	-101.287	83.5444
242.423	524.3709717	158.781	1.19E-07	1.1E-10	35.7715	-101.224	83.5797
242.423	524.5709839	146.523	1.2E-07	1.09E-10	35.9664	-101.162	83.6146
242.423	524.7709961	130.307	1.21E-07	1.07E-10	36.1614	-101.1	83.6492
242.423	524.9710083	110.197	1.21E-07	1.06E-10	36.3565	-101.039	83.6834
242.423	525.1710205	86.2547	1.22E-07	1.05E-10	36.5517	-100.978	83.7173
242.423	525.3709717	58.5416	1.23E-07	1.04E-10	36.7469	-100.919	83.7508
242.423	525.5709839	27.1173	1.23E-07	1.03E-10	36.9421	-100.86	83.784
242.423	525.7709961	-7.95958	1.24E-07	1.01E-10	37.1374	-100.801	83.8168
242.423	525.9710083	-46.6317	1.25E-07	1E-10	37.3327	-100.743	83.8493
242.423	526.1710205	-88.8431	1.25E-07	9.93E-11	37.5281	-100.686	83.8814
242.423	526.3709717	-134.539	1.26E-07	9.82E-11	37.7235	-100.629	83.9132
242.423	526.5709839	176.336	1.27E-07	9.71E-11	37.919	-100.573	83.9447
242.423	526.7709961	123.832	1.27E-07	9.61E-11	38.1146	-100.518	83.9759
242.423	526.9710083	68.0035	1.28E-07	9.5E-11	38.3101	-100.463	84.0068
242.423	527.1710205	8.89933	1.28E-07	9.4E-11	38.5058	-100.409	84.0373
242.423	527.3709717	-53.4303	1.29E-07	9.3E-11	38.7014	-100.355	84.0676
242.423	527.5709839	-118.937	1.3E-07	9.2E-11	38.8971	-100.302	84.0975
243.223	527.7709961	-161.963	1.31E-07	9.03E-11	39.2424	-101.404	84.1496
242.423	527.9710083	100.71	1.31E-07	9E-11	39.2887	-100.197	84.1566
242.423	528.3709717	-51.7894	1.32E-07	8.82E-11	39.6804	-100.094	84.2144
242.423	528.5709839	-132.482	1.33E-07	8.72E-11	39.8763	-100.043	84.243
242.423	528.7709961	143.92	1.34E-07	8.63E-11	40.0723	-99.9932	84.2712
266.623	528.7709961	108.315	1.68E-07	5.31E-11	50.2624	-128.397	85.4354
242.423	529.1710205	-31.8176	1.35E-07	8.46E-11	40.4643	-99.8945	84.3269
242.423	529.3709717	-123.876	1.36E-07	8.37E-11	40.6604	-99.8458	84.3544
242.423	529.5709839	141.326	1.36E-07	8.28E-11	40.8565	-99.7976	84.3815
242.423	529.7709961	43.8282	1.37E-07	8.2E-11	41.0527	-99.7499	84.4085
277.423	529.7709961	151.721	1.94E-07	3.85E-11	58.2637	-136.151	86.0634
242.423	530.1710205	-159.115	1.38E-07	8.04E-11	41.4451	-99.6558	84.4616
242.423	530.3709717	95.5153	1.39E-07	7.95E-11	41.6414	-99.6094	84.4878
242.423	530.5709839	-12.405	1.4E-07	7.87E-11	41.8377	-99.5635	84.5137
243.623	530.7709961	-74.5521	1.41E-07	7.71E-11	42.2481	-101.13	84.5672
242.423	530.9710083	124.246	1.41E-07	7.72E-11	42.2304	-99.4729	84.5649
242.423	531.1710205	8.88629	1.42E-07	7.64E-11	42.4268	-99.4283	84.5901
242.423	531.3709717	-108.884	1.42E-07	7.57E-11	42.6232	-99.384	84.6151
242.423	531.5709839	130.967	1.43E-07	7.49E-11	42.8197	-99.3402	84.6399
242.423	531.7709961	8.47255	1.44E-07	7.42E-11	43.0162	-99.2968	84.6645
242.423	531.9710083	-116.335	1.44E-07	7.35E-11	43.2127	-99.2538	84.6888
242.423	532.1710205	116.575	1.45E-07	7.28E-11	43.4093	-99.2111	84.7129
242.423	532.3709717	-12.7661	1.46E-07	7.21E-11	43.6059	-99.1689	84.7368
242.423	532.5709839	-144.328	1.46E-07	7.14E-11	43.8025	-99.127	84.7605
242.423	532.7709961	81.9189	1.47E-07	7.07E-11	43.9992	-99.0855	84.784
242.423	532.9710083	-53.9961	1.47E-07	7E-11	44.1958	-99.0444	84.8073
278.223	532.9710083	115.78	2.04E-07	3.47E-11	61.0763	-134.503	86.2449
242.423	533.3709717	27.8028	1.49E-07	6.87E-11	44.5893	-98.9633	84.8532
242.423	533.5709839	-114.427	1.49E-07	6.81E-11	44.7861	-98.9233	84.8759

Dataset for user localisation:

AoA	eAoA	loss	phase	ToA	Power	x	y
-132.818	68.5488	89.4299	86.2506	3.65E-08	1.27E-09	242.423	496.971
-133.633	68.8082	89.5466	-110.454	3.69E-08	1.24E-09	242.623	496.971
-134.426	69.0654	89.5189	-99.8663	3.74E-08	1.22E-09	242.823	496.971
-135.198	69.3202	89.3427	123.26	3.78E-08	1.19E-09	243.023	496.971
-135.95	69.5724	89.2644	-155.988	3.82E-08	1.16E-09	243.223	496.971
-136.682	69.8218	89.3476	147.314	3.87E-08	1.13E-09	243.423	496.971
-137.395	70.0683	89.3208	-42.0646	3.92E-08	1.1E-09	243.623	496.971
-138.089	70.3118	89.4575	0.484133	3.96E-08	1.08E-09	243.823	496.971
-138.765	70.5522	89.6283	-80.5856	4.01E-08	1.05E-09	244.023	496.971
-139.422	70.7894	89.789	79.0272	4.06E-08	1.03E-09	244.223	496.971
-140.063	71.0234	89.9909	123.473	4.1E-08	1E-09	244.423	496.971
-140.687	71.254	90.1991	56.7563	4.15E-08	9.79E-10	244.623	496.971
-141.295	71.4812	90.3459	-117.263	4.2E-08	9.56E-10	244.823	496.971
-141.888	71.705	90.3637	-34.8655	4.25E-08	9.33E-10	245.023	496.971
-142.465	71.9254	90.3242	-52.4657	4.3E-08	9.11E-10	245.223	496.971
-143.027	72.1424	90.4421	-166.612	4.35E-08	8.9E-10	245.423	496.971
-143.575	72.3559	90.7021	-13.9816	4.4E-08	8.69E-10	245.623	496.971
-144.109	72.5659	90.7091	48.6256	4.45E-08	8.49E-10	245.823	496.971
-144.63	72.7725	90.7073	24.2882	4.51E-08	8.29E-10	246.023	496.971
-145.138	72.9757	91.0735	-84.0312	4.56E-08	8.1E-10	246.223	496.971
-145.633	73.1755	90.9002	86.5178	4.61E-08	7.91E-10	246.423	496.971
-146.116	73.3719	91.1642	178.677	4.66E-08	7.73E-10	246.623	496.971
-146.587	73.565	91.2349	-164.916	4.72E-08	7.55E-10	246.823	496.971
-147.047	73.7548	91.2773	138.276	4.77E-08	7.38E-10	247.023	496.971
-147.495	73.9413	91.4204	10.6915	4.82E-08	7.21E-10	247.223	496.971
-147.933	74.1246	91.6279	174.678	4.88E-08	7.04E-10	247.423	496.971
-148.361	74.3046	91.3272	-87.5068	4.93E-08	6.89E-10	247.623	496.971
-148.778	74.4816	92.1433	-53.6935	4.99E-08	6.73E-10	247.823	496.971
-149.185	74.6554	91.5895	-81.7939	5.04E-08	6.58E-10	248.023	496.971
-149.583	74.8261	91.6076	-169.8	5.1E-08	6.44E-10	248.223	496.971
-149.972	74.9939	92.4727	44.2206	5.15E-08	6.29E-10	248.423	496.971
-150.352	75.1587	92.3858	-157.875	5.21E-08	6.16E-10	248.623	496.971
-150.723	75.3206	91.7895	-54.2972	5.27E-08	6.02E-10	248.823	496.971
-151.086	75.4797	91.7224	-3.3273	5.32E-08	5.89E-10	249.023	496.971
-151.441	75.6359	92.1562	-3.30932	5.38E-08	5.77E-10	249.223	496.971
-151.788	75.7894	92.7186	-52.6501	5.44E-08	5.64E-10	249.423	496.971
-152.127	75.9402	93.149	-149.816	5.49E-08	5.52E-10	249.623	496.971
-152.459	76.0883	93.4091	66.6683	5.55E-08	5.41E-10	249.823	496.971
-152.783	76.2339	93.5708	-121.775	5.61E-08	5.29E-10	250.023	496.971
-153.101	76.3769	93.6785	6.2225	5.67E-08	5.18E-10	250.223	496.971
-153.411	76.5174	93.6859	91.9787	5.72E-08	5.08E-10	250.423	496.971
-153.716	76.6554	92.6575	136.763	5.78E-08	4.97E-10	250.623	496.971

-154.013	76.7911	92.2912	141.8	5.84E-08	4.87E-10	250.823	496.971
-154.305	76.9243	92.3616	108.266	5.9E-08	4.77E-10	251.023	496.971
-154.59	77.0553	92.7532	37.2983	5.96E-08	4.67E-10	251.223	496.971
-154.87	77.1841	92.6307	-70.0084	6.02E-08	4.58E-10	251.423	496.971
-155.144	77.3106	95.4756	147.401	6.08E-08	4.49E-10	251.623	496.971
-155.412	77.4349	93.7378	-29.4545	6.14E-08	4.4E-10	251.823	496.971
-155.675	77.5572	92.283	120.406	6.19E-08	4.31E-10	252.023	496.971
-155.933	77.6773	93.1696	-122.072	6.25E-08	4.23E-10	252.223	496.971
-156.186	77.7955	95.868	-35.9724	6.31E-08	4.15E-10	252.423	496.971
-156.434	77.9116	92.2201	19.5849	6.37E-08	4.07E-10	252.623	496.971
-156.676	78.0258	92.8312	45.4511	6.43E-08	3.99E-10	252.823	496.971
-156.915	78.1381	95.1615	42.4476	6.49E-08	3.92E-10	253.023	496.971
-157.148	78.2485	96.1749	11.3677	6.55E-08	3.84E-10	253.223	496.971
-157.378	78.3571	96.9438	-47.0227	6.61E-08	3.77E-10	253.423	496.971
-157.603	78.4639	93.311	-131.984	6.67E-08	3.7E-10	253.623	496.971
-157.823	78.569	97.5398	117.199	6.73E-08	3.63E-10	253.823	496.971
-158.04	78.6723	95.4069	-18.7823	6.8E-08	3.56E-10	254.023	496.971
-158.252	78.774	100.273	-179.261	6.86E-08	3.5E-10	254.223	496.971
-158.461	78.874	95.5136	-3.59258	6.92E-08	3.44E-10	254.423	496.971
-158.666	78.9725	95.0958	148.848	6.98E-08	3.37E-10	254.623	496.971
-158.867	79.0693	92.5803	-81.3349	7.04E-08	3.31E-10	254.823	496.971
-159.065	79.1646	92.6272	26.4411	7.1E-08	3.26E-10	255.023	496.971
-159.259	79.2584	99.8595	112.741	7.16E-08	3.2E-10	255.223	496.971
-159.45	79.3508	92.7976	178.112	7.22E-08	3.14E-10	255.423	496.971
-159.638	79.4417	93.297	-136.917	7.28E-08	3.09E-10	255.623	496.971
-159.822	79.5311	99.7956	-111.835	7.35E-08	3.03E-10	255.823	496.971
-160.003	79.6192	93.8505	-106.145	7.41E-08	2.98E-10	256.023	496.971
-160.181	79.706	95.5808	-119.367	7.47E-08	2.93E-10	256.223	496.971
-160.356	79.7914	93.0437	-151.037	7.53E-08	2.88E-10	256.423	496.971
-160.528	79.8755	100.072	159.296	7.59E-08	2.83E-10	256.623	496.971
-160.697	79.9583	95.3678	92.0698	7.65E-08	2.79E-10	256.823	496.971
-160.863	80.0399	93.6279	7.70613	7.72E-08	2.74E-10	257.023	496.971
-161.027	80.1202	94.9051	-93.3844	7.78E-08	2.69E-10	257.223	496.971
-161.187	80.1994	93.8798	149.196	7.84E-08	2.65E-10	257.423	496.971
-161.346	80.2774	97.7204	15.8323	7.9E-08	2.61E-10	257.623	496.971
-161.501	80.3542	100.058	-133.101	7.97E-08	2.56E-10	257.823	496.971
-161.655	80.43	97.3218	62.7593	8.03E-08	2.52E-10	258.023	496.971
-161.806	80.5046	94.1589	-116.236	8.09E-08	2.48E-10	258.223	496.971
-161.954	80.5781	94.837	50.2565	8.15E-08	2.44E-10	258.423	496.971
-162.1	80.6506	96.0473	-157.433	8.22E-08	2.4E-10	258.623	496.971
-162.244	80.722	94.8176	-18.9827	8.28E-08	2.37E-10	258.823	496.971
-162.386	80.7924	95.0411	105.92	8.34E-08	2.33E-10	259.023	496.971
-162.525	80.8618	93.1703	-142.42	8.4E-08	2.29E-10	259.223	496.971
-162.662	80.9303	94.1498	-43.7098	8.47E-08	2.26E-10	259.423	496.971
-162.798	80.9977	93.0334	42.3378	8.53E-08	2.22E-10	259.623	496.971
-162.931	81.0643	94.4049	116.001	8.59E-08	2.19E-10	259.823	496.971

-163.062	81.1299	93.2037	177.55	8.66E-08	2.16E-10	260.023	496.971
-163.191	81.1946	94.6934	-132.752	8.72E-08	2.12E-10	260.223	496.971
-163.319	81.2584	93.5934	-94.6502	8.78E-08	2.09E-10	260.423	496.971
-163.444	81.3214	95.0426	-67.8956	8.85E-08	2.06E-10	260.623	496.971
-163.568	81.3835	95.4354	-52.2469	8.91E-08	2.03E-10	260.823	496.971
-163.69	81.4447	96.4846	-47.4692	8.97E-08	2E-10	261.023	496.971
-163.81	81.5052	100.1	-53.334	9.04E-08	1.97E-10	261.223	496.971
-163.928	81.5648	98.9286	-69.6188	9.1E-08	1.94E-10	261.423	496.971
-164.045	81.6236	100.6	-96.1074	9.16E-08	1.92E-10	261.623	496.971
-164.16	81.6817	97.0671	-132.589	9.23E-08	1.89E-10	261.823	496.971
-164.274	81.739	94.7535	-178.859	9.29E-08	1.86E-10	262.023	496.971
-164.386	81.7956	95.3646	125.282	9.35E-08	1.84E-10	262.223	496.971
-164.496	81.8514	96.2823	60.0286	9.42E-08	1.81E-10	262.423	496.971
-164.605	81.9065	98.9941	-14.43	9.48E-08	1.78E-10	262.623	496.971
-164.713	81.9609	102.752	-97.9096	9.54E-08	1.76E-10	262.823	496.971
-164.819	82.0146	97.0142	169.769	9.61E-08	1.73E-10	263.023	496.971
-164.923	82.0676	93.99	68.7814	9.67E-08	1.71E-10	263.223	496.971
-165.026	82.12	96.6399	-40.7027	9.74E-08	1.69E-10	263.423	496.971
-165.128	82.1717	103.373	-158.517	9.8E-08	1.66E-10	263.623	496.971
-165.228	82.2227	98.5908	75.5002	9.86E-08	1.64E-10	263.823	496.971
-165.327	82.2731	94.6252	-58.4931	9.93E-08	1.62E-10	264.023	496.971
-165.425	82.3229	97.1948	159.657	9.99E-08	1.6E-10	264.223	496.971
-165.522	82.3721	101.805	10.1001	1.01E-07	1.58E-10	264.423	496.971
-165.617	82.4207	97.3542	-147.017	1.01E-07	1.56E-10	264.623	496.971
-165.711	82.4686	95.5443	48.4478	1.02E-07	1.54E-10	264.823	496.971
-165.804	82.516	97.2326	-123.366	1.02E-07	1.52E-10	265.023	496.971
-165.896	82.5629	101.2	57.6777	1.03E-07	1.5E-10	265.223	496.971
-165.986	82.6091	97.3209	-128.289	1.04E-07	1.48E-10	265.423	496.971
-166.076	82.6549	95.4536	38.8634	1.04E-07	1.46E-10	265.623	496.971
-166.164	82.7	100.293	-160.739	1.05E-07	1.44E-10	265.823	496.971
-166.251	82.7447	99.4361	-6.97294	1.06E-07	1.42E-10	266.023	496.971
-166.337	82.7888	95.6573	140.282	1.06E-07	1.4E-10	266.223	496.971
-166.423	82.8324	104.677	-78.857	1.07E-07	1.38E-10	266.423	496.971
-166.507	82.8755	96.8451	55.7249	1.08E-07	1.37E-10	266.623	496.971
-166.59	82.9181	96.4012	-175.86	1.08E-07	1.35E-10	266.823	496.971
-166.672	82.9602	102.803	-53.503	1.09E-07	1.33E-10	267.023	496.971
-166.753	83.0019	95.8469	62.9035	1.1E-07	1.32E-10	267.223	496.971
-166.833	83.043	99.664	173.464	1.1E-07	1.3E-10	267.423	496.971
-166.912	83.0837	99.1082	-81.7206	1.11E-07	1.28E-10	267.623	496.971
-166.99	83.124	97.5111	17.4507	1.11E-07	1.27E-10	267.823	496.971
-167.068	83.1637	99.8568	111.075	1.12E-07	1.25E-10	268.023	496.971
-167.144	83.2031	98.4389	-160.753	1.13E-07	1.24E-10	268.223	496.971
-167.22	83.242	96.6086	-77.9391	1.13E-07	1.22E-10	268.423	496.971
-167.294	83.2805	103.363	-0.39297	1.14E-07	1.21E-10	268.623	496.971
-167.368	83.3185	95.5098	71.9746	1.15E-07	1.19E-10	268.823	496.971
-167.441	83.3561	107.769	139.251	1.15E-07	1.18E-10	269.023	496.971

-167.513	83.3934	95.6327	-158.48	1.16E-07	1.17E-10	269.223	496.971
-167.584	83.4302	102.804	-101.133	1.17E-07	1.15E-10	269.423	496.971
-167.655	83.4666	96.4584	-48.6275	1.17E-07	1.14E-10	269.623	496.971
-167.725	83.5027	98.7447	-0.88397	1.18E-07	1.13E-10	269.823	496.971
-167.794	83.5383	98.3643	42.1759	1.19E-07	1.11E-10	270.023	496.971
-167.862	83.5736	96.5209	80.6284	1.19E-07	1.1E-10	270.223	496.971
-167.929	83.6085	101.853	114.548	1.2E-07	1.09E-10	270.423	496.971
-167.996	83.643	95.7791	144.009	1.21E-07	1.08E-10	270.623	496.971
-168.062	83.6772	105.731	169.081	1.21E-07	1.06E-10	270.823	496.971
-168.128	83.711	96.4655	-170.164	1.22E-07	1.05E-10	271.023	496.971
-168.192	83.7445	104.223	-153.658	1.22E-07	1.04E-10	271.223	496.971
-168.256	83.7776	98.3255	-141.335	1.23E-07	1.03E-10	271.423	496.971
-168.319	83.8104	101.799	-133.127	1.24E-07	1.02E-10	271.623	496.971
-168.382	83.8428	98.8962	-128.971	1.24E-07	1.01E-10	271.823	496.971
-168.444	83.8749	101.368	-128.804	1.25E-07	9.95E-11	272.023	496.971
-168.505	83.9067	96.9215	-132.563	1.26E-07	9.84E-11	272.223	496.971
-168.566	83.9382	103.44	-140.188	1.26E-07	9.73E-11	272.423	496.971
-168.626	83.9694	96.6686	-151.62	1.27E-07	9.63E-11	272.623	496.971
-168.685	84.0002	102.187	-166.801	1.28E-07	9.52E-11	272.823	496.971
-132.064	68.8281	99.8501	174.327	1.28E-07	9.42E-11	242.423	497.171
-131.331	69.1036	97.5822	151.82	1.29E-07	9.32E-11	242.423	497.371
-130.619	69.3754	100.478	125.731	1.3E-07	9.22E-11	242.423	497.571
-129.927	69.6432	97.5421	96.1156	1.3E-07	9.12E-11	242.423	497.771
-129.254	69.9071	100.196	63.0256	1.31E-07	9.03E-11	242.423	497.971
-128.601	70.1668	98.1439	26.5126	1.32E-07	8.93E-11	242.423	498.171
-164.437	82.9413	105.096	-13.3726	1.32E-07	8.84E-11	266.623	498.171
-127.347	70.674	95.9242	-56.5806	1.33E-07	8.75E-11	242.423	498.571
-128.301	71.2874	105.278	-103.063	1.34E-07	8.65E-11	242.823	498.771
-126.161	71.1645	99.969	-152.771	1.34E-07	8.56E-11	242.423	498.971
-125.592	71.4035	97.9791	154.341	1.35E-07	8.48E-11	242.423	499.171
-125.039	71.6384	101.645	98.3202	1.36E-07	8.39E-11	242.423	499.371
-124.5	71.8691	98.9841	39.2104	1.36E-07	8.3E-11	242.423	499.571
-123.976	72.0956	103.825	-22.9436	1.37E-07	8.22E-11	242.423	499.771
-123.466	72.3181	97.5126	-88.0986	1.37E-07	8.14E-11	242.423	499.971
-122.969	72.5366	103.904	-156.212	1.38E-07	8.06E-11	242.423	500.171
-122.485	72.7511	102.577	132.758	1.39E-07	7.97E-11	242.423	500.371
-122.013	72.9616	97.3542	58.8526	1.39E-07	7.9E-11	242.423	500.571
-121.554	73.1682	110.345	-17.8882	1.4E-07	7.82E-11	242.423	500.771
-121.106	73.371	100.397	-97.4249	1.41E-07	7.74E-11	242.423	500.971
-120.669	73.57	99.5077	-179.719	1.41E-07	7.66E-11	242.423	501.171
-120.244	73.7652	102	95.2685	1.42E-07	7.59E-11	242.423	501.371
-119.829	73.9569	100.069	7.57411	1.43E-07	7.51E-11	242.423	501.571
-119.424	74.1449	104.808	-82.7652	1.43E-07	7.44E-11	242.423	501.771
-119.029	74.3294	99.3458	-175.713	1.44E-07	7.37E-11	242.423	501.971
-118.644	74.5104	99.6655	88.765	1.45E-07	7.3E-11	242.423	502.171
-118.268	74.688	116.199	-9.29539	1.45E-07	7.23E-11	242.423	502.371

-117.901	74.8623	89.0233	-109.86	1.46E-07	7.16E-11	242.423	502.571
-117.543	75.0334	88.8389	-104.189	3.7E-08	1.24E-09	242.423	502.771
-117.193	75.2012	89.5143	-70.1938	3.74E-08	1.21E-09	242.423	502.971
-117.193	75.2012	89.6067	-166.773	3.79E-08	1.18E-09	242.423	502.971
-116.851	75.3659	89.2205	-29.1161	3.84E-08	1.15E-09	242.423	503.171
-116.517	75.5275	89.3805	-12.5912	3.89E-08	1.12E-09	242.423	503.371
-116.517	75.5275	96.2851	-112.74	3.93E-08	1.09E-09	242.423	503.371
-116.191	75.6861	90.0418	121.846	1.09E-07	1.34E-10	242.423	503.571
-115.872	75.8418	89.9563	73.9255	4.03E-08	1.04E-09	242.423	503.771
-161.204	84.8383	90.2611	-45.9798	4.16E-08	9.76E-10	277.423	503.771
-115.255	76.1445	90.3426	-156.766	4.13E-08	9.88E-10	242.423	504.171
-114.957	76.2918	90.389	-59.1956	4.19E-08	9.64E-10	242.423	504.371
-114.665	76.4363	90.4786	-54.9496	4.24E-08	9.4E-10	242.423	504.571
-114.38	76.5782	90.4746	-140.657	4.29E-08	9.17E-10	242.423	504.771
-114.101	76.7175	90.4888	46.9181	4.34E-08	8.94E-10	242.423	504.971
-113.828	76.8543	90.6084	150.882	4.39E-08	8.73E-10	242.423	505.171
-113.56	76.9886	90.9121	174.216	4.45E-08	8.51E-10	242.423	505.371
-113.298	77.1205	90.9881	119.779	4.5E-08	8.31E-10	242.423	505.571
-113.042	77.2501	90.8374	-9.68322	4.56E-08	8.11E-10	242.423	505.771
-112.791	77.3773	91.1836	148.463	4.61E-08	7.91E-10	242.423	505.971
-112.545	77.5023	91.3252	-123.256	4.66E-08	7.73E-10	242.423	506.171
-112.304	77.6252	91.0836	-102.415	4.72E-08	7.54E-10	242.423	506.371
-112.068	77.7458	91.7475	-146.688	4.77E-08	7.37E-10	242.423	506.571
-111.836	77.8644	91.2164	106.159	4.83E-08	7.19E-10	242.423	506.771
-111.609	77.9809	92.0035	-61.7314	4.89E-08	7.03E-10	242.423	506.971
-111.387	78.0954	91.4426	71.6973	4.94E-08	6.86E-10	242.423	507.171
-111.169	78.2079	91.9267	148.42	5E-08	6.71E-10	242.423	507.371
-110.955	78.3185	92.2559	170.331	5.05E-08	6.55E-10	242.423	507.571
-110.745	78.4273	91.5336	139.251	5.11E-08	6.41E-10	242.423	507.771
-156.454	85.0007	92.0644	56.9272	5.17E-08	6.26E-10	277.423	507.771
-110.337	78.6393	92.0644	-74.9618	5.23E-08	6.12E-10	242.423	508.171
-110.139	78.7427	92.9043	-74.9618	5.23E-08	6.12E-10	242.423	508.371
-109.945	78.8443	92.5276	105.196	5.28E-08	5.99E-10	242.423	508.571
-109.754	78.9443	92.5276	-121.05	5.34E-08	5.85E-10	242.423	508.771
-109.566	79.0426	91.9681	-121.05	5.34E-08	5.85E-10	242.423	508.971
-109.382	79.1394	91.9116	-32.2128	5.4E-08	5.73E-10	242.423	509.171
-109.201	79.2345	102.047	13.1392	5.46E-08	5.6E-10	242.423	509.371
-109.024	79.3282	92.4662	-70.1522	1.48E-07	6.91E-11	242.423	509.571
-108.85	79.4203	92.9109	-21.1671	5.57E-08	5.36E-10	242.423	509.771
-154.197	85.0899	92.9196	-98.2324	5.63E-08	5.25E-10	277.423	509.771
-108.51	79.6002	92.9964	146.407	5.69E-08	5.14E-10	242.423	510.171
-108.344	79.688	92.8512	-6.07178	5.75E-08	5.03E-10	242.423	510.371
-108.182	79.7745	92.5089	165.462	5.81E-08	4.92E-10	242.423	510.571
-108.022	79.8596	92.3275	-57.9024	5.87E-08	4.82E-10	242.423	510.771
-107.865	79.9434	92.6943	44.8838	5.93E-08	4.72E-10	242.423	510.971
-107.71	80.0259	93.8377	114.83	5.99E-08	4.63E-10	242.423	511.171

-107.558	80.1071	94.756	152.908	6.05E-08	4.53E-10	242.423	511.371
-107.409	80.1871	93.5511	160.055	6.11E-08	4.44E-10	242.423	511.571
-107.262	80.2659	92.6243	137.173	6.17E-08	4.35E-10	242.423	511.771
-107.117	80.3435	93.939	85.1304	6.23E-08	4.27E-10	242.423	511.971
-106.975	80.42	94.9213	4.76641	6.29E-08	4.18E-10	242.423	512.171
-106.835	80.4953	92.8245	-103.111	6.35E-08	4.1E-10	242.423	512.371
-106.697	80.5695	94.395	122.276	6.41E-08	4.02E-10	242.423	512.571
-106.561	80.6427	94.5657	-38.3194	6.47E-08	3.94E-10	242.423	512.771
-106.428	80.7147	93.0858	135.827	6.53E-08	3.87E-10	242.423	512.971
-106.296	80.7857	95.7566	-74.5857	6.59E-08	3.8E-10	242.423	513.171
-106.167	80.8557	103	51.1184	6.65E-08	3.72E-10	242.423	513.371
-106.039	80.9247	96.0497	171.124	1.53E-07	6.46E-11	242.423	513.571
-105.914	80.9927	93.1547	-126.539	6.78E-08	3.59E-10	242.423	513.771
-105.79	81.0598	96.2606	-68.6623	6.84E-08	3.52E-10	242.423	513.971
-105.669	81.1259	93.4097	-32.1929	6.9E-08	3.46E-10	242.423	514.171
-105.549	81.1911	95.5627	-16.5631	6.96E-08	3.39E-10	242.423	514.371
-105.431	81.2554	94.7591	-21.2243	7.02E-08	3.33E-10	242.423	514.571
-105.314	81.3187	93.7786	-45.6465	7.08E-08	3.27E-10	242.423	514.771
-105.2	81.3813	96.8782	-89.3171	7.15E-08	3.21E-10	242.423	514.971
-105.087	81.4429	94.1962	-151.74	7.21E-08	3.16E-10	242.423	515.171
-104.975	81.5037	98.5785	127.563	7.27E-08	3.1E-10	242.423	515.371
-104.865	81.5638	97.1086	-31.7422	1.56E-07	6.21E-11	242.423	515.571
-104.757	81.6229	95.292	-86.8092	7.39E-08	2.99E-10	242.423	515.771
-104.65	81.6814	93.7173	140.399	7.46E-08	2.94E-10	242.423	515.971
-104.545	81.739	95.2185	-8.89895	7.52E-08	2.89E-10	242.423	516.171
-104.442	81.7959	97.6449	-174.294	7.58E-08	2.84E-10	242.423	516.371
-104.339	81.852	96.2094	4.60646	7.64E-08	2.79E-10	242.423	516.571
-104.238	81.9074	94.297	168.186	7.71E-08	2.75E-10	242.423	516.771
-104.139	81.962	94.0376	-43.1856	7.77E-08	2.7E-10	242.423	516.971
-104.041	82.016	95.1853	90.8505	7.83E-08	2.66E-10	242.423	517.171
-103.944	82.0693	97.0839	-149.358	7.89E-08	2.61E-10	242.423	517.371
-103.848	82.1219	98.3332	-43.4738	7.96E-08	2.57E-10	242.423	517.571
-103.754	82.1738	97.8523	48.8298	8.02E-08	2.53E-10	242.423	517.771
-103.661	82.2251	96.6365	127.87	8.08E-08	2.49E-10	242.423	517.971
-103.569	82.2757	95.6287	-166.045	8.15E-08	2.45E-10	242.423	518.171
-103.479	82.3257	94.9982	-112.618	8.21E-08	2.41E-10	242.423	518.371
-103.389	82.3751	94.6663	-71.5591	8.27E-08	2.37E-10	242.423	518.571
-103.301	82.4238	94.527	-42.5865	8.34E-08	2.33E-10	242.423	518.771
-103.214	82.472	94.4956	-25.4277	8.4E-08	2.3E-10	242.423	518.971
-103.128	82.5196	94.5182	-19.8179	8.46E-08	2.26E-10	242.423	519.171
-103.043	82.5666	94.5728	-25.4997	8.53E-08	2.23E-10	242.423	519.371
-102.959	82.613	94.6682	-42.2232	8.59E-08	2.19E-10	242.423	519.571
-102.877	82.6589	94.8436	-69.7457	8.65E-08	2.16E-10	242.423	519.771
-144.169	85.5762	95.1674	-107.831	8.72E-08	2.13E-10	277.423	519.771
-102.714	82.749	95.7358	-156.251	8.78E-08	2.09E-10	242.423	520.171
-102.634	82.7932	96.6616	145.219	8.84E-08	2.06E-10	242.423	520.371

-102.556	82.837	98.015	76.7945	8.91E-08	2.03E-10	242.423	520.571
-102.478	82.8802	99.5408	-1.31391	8.97E-08	2E-10	242.423	520.771
-102.401	82.9229	100.031	-88.9012	9.03E-08	1.97E-10	242.423	520.971
-102.325	82.9651	98.5584	174.232	9.1E-08	1.94E-10	242.423	521.171
-102.25	83.0069	96.5474	68.279	9.16E-08	1.92E-10	242.423	521.371
-102.176	83.0481	95.2595	-46.5711	9.23E-08	1.89E-10	242.423	521.571
-102.103	83.0889	95.1544	-170.135	9.29E-08	1.86E-10	242.423	521.771
-102.03	83.1292	96.5521	57.766	9.35E-08	1.84E-10	242.423	521.971
-101.959	83.1691	99.5093	-82.6943	9.42E-08	1.81E-10	242.423	522.171
-101.888	83.2085	100.354	128.653	9.48E-08	1.78E-10	242.423	522.371
-101.818	83.2475	97.1071	-28.026	9.55E-08	1.76E-10	242.423	522.571
-101.749	83.2861	95.3264	167.428	9.61E-08	1.73E-10	242.423	522.771
-101.681	83.3242	96.1734	-4.82835	9.67E-08	1.71E-10	242.423	522.971
-101.613	83.3619	99.8641	175.357	9.74E-08	1.69E-10	242.423	523.171
-101.547	83.3992	99.9908	-11.8663	9.8E-08	1.66E-10	242.423	523.371
-101.481	83.4361	96.1463	153.645	9.87E-08	1.64E-10	242.423	523.571
-101.415	83.4726	95.782	-47.9673	9.93E-08	1.62E-10	242.423	523.771
-101.351	83.5087	99.55	103.434	9.99E-08	1.6E-10	242.423	523.971
-101.287	83.5444	100.167	-112.017	1.01E-07	1.58E-10	242.423	524.171
-101.224	83.5797	95.9697	25.8095	1.01E-07	1.55E-10	242.423	524.371
-101.162	83.6146	96.6455	157.042	1.02E-07	1.53E-10	242.423	524.571
-101.1	83.6492	101.783	-78.1958	1.03E-07	1.51E-10	242.423	524.771
-101.039	83.6834	97.5787	40.2175	1.03E-07	1.49E-10	242.423	524.971
-100.978	83.7173	95.9229	152.4	1.04E-07	1.47E-10	242.423	525.171
-100.919	83.7508	108.149	-101.533	1.04E-07	1.46E-10	242.423	525.371
-100.86	83.784	98.7258	-92.4635	1.73E-07	4.96E-11	242.423	525.571
-100.801	83.8168	95.9261	92.7039	1.06E-07	1.42E-10	242.423	525.771
-100.743	83.8493	100.731	-178.91	1.06E-07	1.4E-10	242.423	525.971
-100.686	83.8814	98.6018	-96.2043	1.07E-07	1.38E-10	242.423	526.171
-100.629	83.9132	96.1877	-19.0773	1.08E-07	1.37E-10	242.423	526.371
-100.573	83.9447	102.162	52.571	1.08E-07	1.35E-10	242.423	526.571
-100.518	83.9759	97.4001	118.838	1.09E-07	1.33E-10	242.423	526.771
-100.463	84.0068	97.205	179.82	1.1E-07	1.31E-10	242.423	526.971
-100.409	84.0373	102.472	-124.392	1.1E-07	1.3E-10	242.423	527.171
-100.355	84.0676	96.279	-73.7051	1.11E-07	1.28E-10	242.423	527.371
-100.302	84.0975	100.404	-28.0314	1.12E-07	1.27E-10	242.423	527.571
-101.404	84.1496	98.6015	12.7161	1.12E-07	1.25E-10	243.223	527.771
-100.197	84.1566	97.0997	48.6223	1.13E-07	1.24E-10	242.423	527.971
-100.094	84.2144	102.749	79.7701	1.14E-07	1.22E-10	242.423	528.371
-100.043	84.243	96.3807	106.241	1.14E-07	1.21E-10	242.423	528.571
-99.9932	84.2712	102.436	128.113	1.15E-07	1.19E-10	242.423	528.771
-128.397	85.4354	97.2922	145.465	1.15E-07	1.18E-10	266.623	528.771
-99.8945	84.3269	99.443	158.373	1.16E-07	1.16E-10	242.423	529.171
-99.8458	84.3544	99.2101	166.91	1.17E-07	1.15E-10	242.423	529.371
-99.7976	84.3815	97.7152	171.149	1.17E-07	1.14E-10	242.423	529.571
-99.7499	84.4085	101.534	171.161	1.18E-07	1.12E-10	242.423	529.771

-136.151	86.0634	96.9712	167.016	1.19E-07	1.11E-10	277.423	529.771
-99.6558	84.4616	103.431	158.781	1.19E-07	1.1E-10	242.423	530.171
-99.6094	84.4878	96.7572	146.523	1.2E-07	1.09E-10	242.423	530.371
-99.5635	84.5137	104.302	130.307	1.21E-07	1.07E-10	242.423	530.571
-101.13	84.5672	96.7785	110.197	1.21E-07	1.06E-10	243.623	530.771
-99.4729	84.5649	104.491	86.2547	1.22E-07	1.05E-10	242.423	530.971
-99.4283	84.5901	96.8608	58.5416	1.23E-07	1.04E-10	242.423	531.171
-99.384	84.6151	104.609	27.1173	1.23E-07	1.03E-10	242.423	531.371
-99.3402	84.6399	96.9286	-7.95958	1.24E-07	1.01E-10	242.423	531.571
-99.2968	84.6645	104.831	-46.6317	1.25E-07	1E-10	242.423	531.771
-99.2538	84.6888	96.9956	-88.8431	1.25E-07	9.93E-11	242.423	531.971
-99.2111	84.7129	104.822	-134.539	1.26E-07	9.82E-11	242.423	532.171
-99.1689	84.7368	97.1586	176.336	1.27E-07	9.71E-11	242.423	532.371
-99.127	84.7605	103.912	123.832	1.27E-07	9.61E-11	242.423	532.571
-99.0855	84.784	97.5951	68.0035	1.28E-07	9.5E-11	242.423	532.771
-99.0444	84.8073	102.019	8.89933	1.28E-07	9.4E-11	242.423	532.971
-134.503	86.2449	98.5774	-53.4303	1.29E-07	9.3E-11	278.223	532.971
-98.9633	84.8532	103.455	-118.937	1.3E-07	9.2E-11	242.423	533.371
-98.9233	84.8759	100.516	-161.963	1.31E-07	9.03E-11	242.423	533.571
-168.744	84.0308	103.823	100.71	1.31E-07	9E-11	273.023	496.971
-168.802	84.061	97.4184	-51.7894	1.32E-07	8.82E-11	273.223	496.971
-168.86	84.0909	105.578	-132.482	1.33E-07	8.72E-11	273.423	496.971
-168.917	84.1206	102.463	143.92	1.34E-07	8.63E-11	273.623	496.971
-168.973	84.1499	101.615	108.315	1.68E-07	5.31E-11	273.823	496.971
-169.029	84.179	100.131	-31.8176	1.35E-07	8.46E-11	274.023	496.971
-169.084	84.2078	98.4904	-123.876	1.36E-07	8.37E-11	274.223	496.971
-169.139	84.2363	105.038	141.326	1.36E-07	8.28E-11	274.423	496.971
-169.193	84.2645	102.148	43.8282	1.37E-07	8.2E-11	274.623	496.971
-169.247	84.2925	104.956	151.721	1.94E-07	3.85E-11	274.823	496.971
-169.3	84.3202	98.6272	-159.115	1.38E-07	8.04E-11	275.023	496.971
-169.353	84.3477	98.1606	95.5153	1.39E-07	7.95E-11	275.223	496.971
-169.405	84.3748	98.1228	-12.405	1.4E-07	7.87E-11	275.423	496.971
-169.456	84.4018	98.1611	-74.5521	1.41E-07	7.71E-11	275.623	496.971
-169.508	84.4284	103.123	124.246	1.41E-07	7.72E-11	275.823	496.971
-169.558	84.4549	101.69	8.88629	1.42E-07	7.64E-11	276.023	496.971
-169.608	84.4811	98.0277	-108.884	1.42E-07	7.57E-11	276.223	496.971
-169.658	84.507	104.464	130.967	1.43E-07	7.49E-11	276.423	496.971
-169.707	84.5327	97.2577	8.47255	1.44E-07	7.42E-11	276.623	496.971
-169.756	84.5582	101.474	-116.335	1.44E-07	7.35E-11	276.823	496.971
-169.804	84.5834	107.899	116.575	1.45E-07	7.28E-11	277.023	496.971
-169.852	84.6084	96.9485	-12.7661	1.46E-07	7.21E-11	277.223	496.971
-169.9	84.6332	104.712	-144.328	1.46E-07	7.14E-11	277.423	496.971
-169.947	84.6578	102.726	81.9189	1.47E-07	7.07E-11	277.623	496.971
-169.993	84.6821	98.9729	-53.9961	1.47E-07	7E-11	277.823	496.971
-170.039	84.7062	103.305	115.78	2.04E-07	3.47E-11	278.023	496.971
-170.085	84.7302	101.439	27.8028	1.49E-07	6.87E-11	278.223	496.971

-170.13	84.7539	496.971	-114.427	1.49E-07	6.81E-11